VTRC
Virginia Transportation Research Council

We Bring Innovation to Transportation

Implementation of an Improved Shear Key Detail in the Buffalo Branch Bridge

http://www.virginiadot.org/vtrc/main/online_reports/pdf/20-r4.pdf

CARRIE FIELD
Senior Associate
Data Analytics, PwC

CARIN L. ROBERTS-WOLLMANN, Ph.D., P.E.
Professor
Via Department of Civil and Environmental Engineering
Virginia Tech

THOMAS E. COUSINS, Ph.D., P.E.
Professor
Glenn Department of Civil Engineering
Clemson University

Final Report VTRC 20-R4

VIRGINIA TRANSPORTATION RESEARCH COUNCIL
530 Edgemont Road, Charlottesville, VA 22903-2454
vtrc.virginiadot.org

Standard Title Page - Report on Federally Funded Project

1. Report No.: FHWA/VTRC 20-R4	2. Government Accession No.:	3. Recipient's Catalog No.:
4. Title and Subtitle: Implementation of an Improved Shear Key Detail in the Buffalo Branch Bridge		5. Report Date: May 2020 6. Performing Organization Code:
7. Author(s): Carrie Field, Carin L. Roberts-Wollmann, Ph.D., P.E., and Thomas E. Cousins, Ph.D., P.E.		8. Performing Organization Report No.: VTRC 20-R4
9. Performing Organization and Address: Virginia Transportation Research Council 530 Edgemont Road Charlottesville, VA 22903		10. Work Unit No. (TRAIS): 11. Contract or Grant No.: 105794
12. Sponsoring Agencies' Name and Address: Virginia Department of Transportation 1401 E. Broad Street Richmond, VA 23219 Federal Highway Administration 400 North 8th Street, Room 750 Richmond, VA 23219-4825		13. Type of Report and Period Covered: Final Contract 14. Sponsoring Agency Code:
15. Supplementary Notes: This is an SPR-2 report.		

16. Abstract:

Adjacent box beam bridges are economical bridge systems for accelerated bridge construction. The box beams are constructed at precast plants and are traditionally connected by a shear key filled with grout. This system is typically used for short spans with low clearance restrictions. However, due to the grout deteriorating and debonding from the precast concrete in the shear key, reflective cracking propagates through the deck, which allows water and chemicals to leak down into the joints. This can lead to corrosion of the reinforcing and prestressing steel inside the precast member. This necessitates the bridge being rehabilitated or replaced, which negates some of the economic advantage it had to begin with.

This research project aimed to design a rehabilitation plan for an adjacent box beam bridge with deteriorated joints using very high performance concrete (VHPC). VHPC was chosen as an economical alternative to the proprietary ultra high performance concrete (UHPC) and extensive material tests were performed. The less expensive VHPC generally performed slightly below UHPC; however, compared to conventional grout, VHPC had higher compressive and tensile strengths, a higher modulus of elasticity, gained strength faster, bonded better to precast concrete, was more durable over time, and shrank less. The rehabilitation also included pockets cut into the beams across the joints, which are referred to as cutouts. A short reinforcing bar was placed in each cutout, and the cutouts were filled with VHPC along with the shear key.

The repair method developed in this research project was used to rehabilitate the Buffalo Branch Bridge. Live load tests were performed before and after the rehabilitation to determine if the new connection detail resulted in better load distribution and smaller relative displacements of adjacent beams. Strain and displacement measurements indicated that the soffit beams were more engaged in carrying truck loads after the repair, and relative vertical displacements of adjacent boxes were much smaller.

17 Key Words: longitudinal joints, shear key, grout, high performance concrete adjacent precast concrete member, retrofit, load distribution	18. Distribution Statement: No restrictions. This document is available to the public through NTIS, Springfield, VA 22161.		
19. Security Classif. (of this report): Unclassified	20. Security Classif. (of this page): Unclassified	21. No. of Pages: 73	22. Price:

Form DOT F 1700.7 (8-72) Reproduction of completed page authorized

FINAL REPORT

IMPLEMENTATION OF AN IMPROVED SHEAR KEY DETAIL IN THE BUFFALO BRANCH BRIDGE

Carrie Field
Senior Associate
Data Analytics, PwC

Carin L. Roberts-Wollmann, Ph.D., P.E.
Professor
Via Department of Civil and Environmental Engineering
Virginia Tech

Thomas E. Cousins, Ph.D., P.E.
Professor
Glenn Department of Civil Engineering
Clemson University

Project Manager
Bernie Kassner, Ph.D., P.E., Virginia Transportation Research Council

In Cooperation with the U.S. Department of Transportation
Federal Highway Administration

Virginia Transportation Research Council
(A partnership of the Virginia Department of Transportation
and the University of Virginia since 1948)

Charlottesville, Virginia

May 2019
VTRC 20-R4

DISCLAIMER

The project that is the subject of this report was done under contract for the Virginia Department of Transportation, Virginia Transportation Research Council. The contents of this report reflect the views of the authors, who are responsible for the facts and the accuracy of the data presented herein. The contents do not necessarily reflect the official views or policies of the Virginia Department of Transportation, the Commonwealth Transportation Board, or the Federal Highway Administration. This report does not constitute a standard, specification, or regulation. Any inclusion of manufacturer names, trade names, or trademarks is for identification purposes only and is not to be considered an endorsement.

Each contract report is peer reviewed and accepted for publication by staff of the Virginia Transportation Research Council with expertise in related technical areas. Final editing and proofreading of the report are performed by the contractor.

ABSTRACT

Adjacent box beam bridges are economical bridge systems for accelerated bridge construction. The box beams are constructed at precast plants and are traditionally connected by a shear key filled with grout. This system is typically used for short spans with low clearance restrictions. However, due to the grout deteriorating and debonding from the precast concrete in the shear key, reflective cracking propagates through the deck, which allows water and chemicals to leak down into the joints. This can lead to corrosion of the reinforcing and prestressing steel inside the precast member. This necessitates the bridge being rehabilitated or replaced, which negates some of the economic advantage it had to begin with.

This research project aimed to design a rehabilitation plan for an adjacent box beam bridge with deteriorated joints using very high performance concrete (VHPC). VHPC was chosen as an economical alternative to the proprietary ultra high performance concrete (UHPC) and extensive material tests were performed. The less expensive VHPC generally performed slightly below UHPC; however, compared to conventional grout, VHPC had higher compressive and tensile strengths, a higher modulus of elasticity, gained strength faster, bonded better to precast concrete, was more durable over time, and shrank less. The rehabilitation also included pockets cut into the beams across the joints, which are referred to as cutouts. A short reinforcing bar was placed in each cutout, and the cutouts were filled with VHPC along with the shear key.

The repair method developed in this research project was used to rehabilitate the Buffalo Branch Bridge. Live load tests were performed before and after the rehabilitation to determine if the new connection detail resulted in better load distribution and smaller relative displacements of adjacent beams. Strain and displacement measurements indicated that the soffit beams were more engaged in carrying truck loads after the repair, and relative vertical displacements of adjacent boxes were much smaller.

FINAL REPORT

IMPLEMENTATION OF AN IMPROVED SHEAR KEY DETAIL IN THE BUFFALO BRANCH BRIDGE

Carrie Field
Senior Associate
Data Analytics, PwC

Carin L. Roberts-Wollmann, Ph.D., P.E.
Professor
Via Department of Civil and Environmental Engineering
Virginia Tech

Thomas E. Cousins, Ph.D., P.E.
Professor
Glenn Department of Civil Engineering
Clemson University

INTRODUCTION

Motivation

Adjacent prestressed girder bridges are comprised of either precast adjacent box beams or voided slab sections as the superstructure, with either an asphalt topping or additional concrete deck placed directly on top. The precast members are traditionally connected with a longitudinal shear key filled with grout and transversely tied at intermittent diaphragm locations. This shear key enhances transverse load transfer between neighboring adjacent members. By using precast members, these bridges are fairly simple and can be rapidly constructed. Adjacent prestressed member bridges are an efficient design for short spans and bridge locations with low vertical clearance requirements. Furthermore, the precast concrete box beams also provide a smooth bottom, which allows greater passage of debris under the bridge during flooding compared to beam/girder spans.

However, over time, the traditional grout shear key tends to deteriorate, causing reflective cracking to propagate through the deck and into the wearing surface, as shown in Figure 1. These reflective cracks allow water and corrosive agents, such as deicer salts, to penetrate down into the joints, an example of which can be seen in Figure 2, which is the underside of the joint in Figure 1. If left uncorrected, chloride-ladened water can eventually cause the reinforcing and prestressing steel in the precast members to corrode. This corrosion leads to the need for bridge repair or replacement well before the end of its anticipated design life, negating the assessed economic value of the adjacent member system.

Graybeal (2014) suggested replacing the grout shear key with ultra high performance concrete (UHPC), defined as “a cementitious composite material composed of an optimized

Figure 1. Reflective Cracking

Figure 2. Leaking Joint

gradation of granular constituents, a water-to-cementitious materials ratio less than 0.25, and a high percentage of discontinuous internal [steel] fiber reinforcement. The mechanical properties of UHPC include compressive strength greater than 21.7 ksi and sustained post-cracking tensile strength greater than 0.72 ksi. Additionally Graybeal asserted that the discontinuous pore structure of UHPC significantly enhances the durability compared to traditional concrete or grout because the material reduces the liquid ingress. Most UHPC materials are proprietary and come in premix bags. Graybeal's recommendation for a UHPC connection of adjacent box beams is shown in Figure 3.

In Graybeal's connection, the adjacent members are formed at the precast plant with reinforcing steel extending into the shear key every 8 in. When the precast members are placed in the field, the overlapping reinforcing steel is spliced together, eliminating the need for transverse post-tensioning. The joint is then filled with UHPC instead of grout, ultimately allowing the top flange of the box beams to act as a continuous slab.

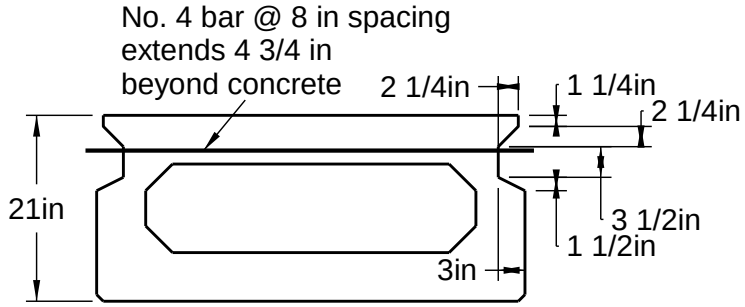

Figure 3. Graybeal's UHPC Adjacent Box Beam Connection

Previous research done at Virginia Tech by Halbe (2014) developed a very similar design compared to Graybeal's. However, instead of designing the connection exclusively for new construction, the objective was to design a connection that could be also be used to rehabilitate existing bridges. The recommended connection design from Halbe (2014) is shown in Figure 4. It specifies either using UHPC or Virginia Tech's more economical very high performance concrete (VHPC). In the retrofit, the blockout is saw-cut into the existing boxes, rather than formed, and the reinforcing bar is not in direct contact with a reinforcing bar in the box beam.

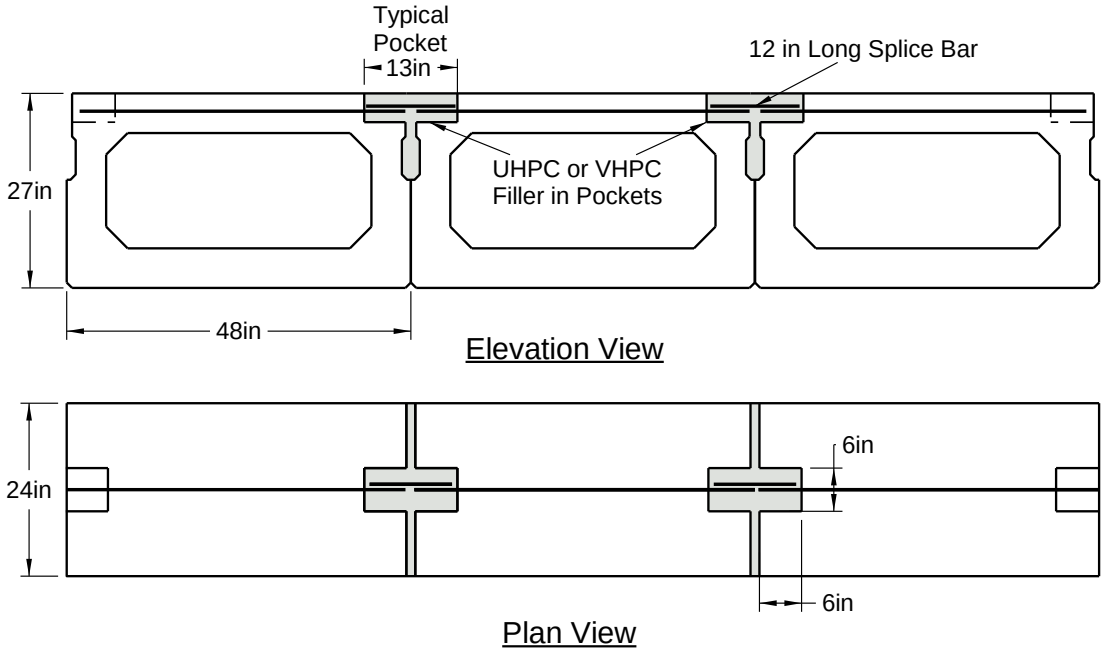

Figure 4. Halbe's UHPC/VHPC Adjacent Box Beam Connection

Background

Overview of Buffalo Branch Bridge

The most recent visual inspection of the Buffalo Branch Bridge performed by the Virginia Department of Transportation (VDOT) in January 2014 stated that water and efflorescence were seeping through the entire length of the furthest downstream joint. Evidence

of leakage was also seen on the second downstream joint and the furthest upstream joint within 6 ft of the abutments. The leaking downstream joint is shown in Figure 2. The plan and transverse views of the bridge plans are shown in Figure 5 and Figure 6. The 55-ft span bridge consists of nine simply supported adjacent box beams with transverse ties at the third points.

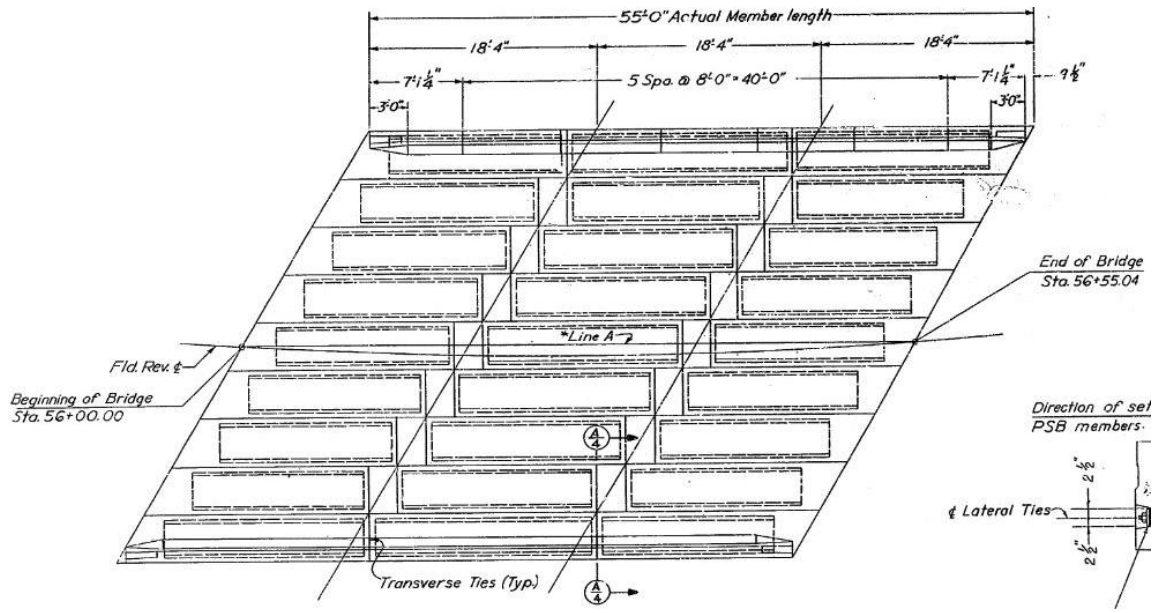

Figure 5. Plan View of Buffalo Branch Bridge Plans

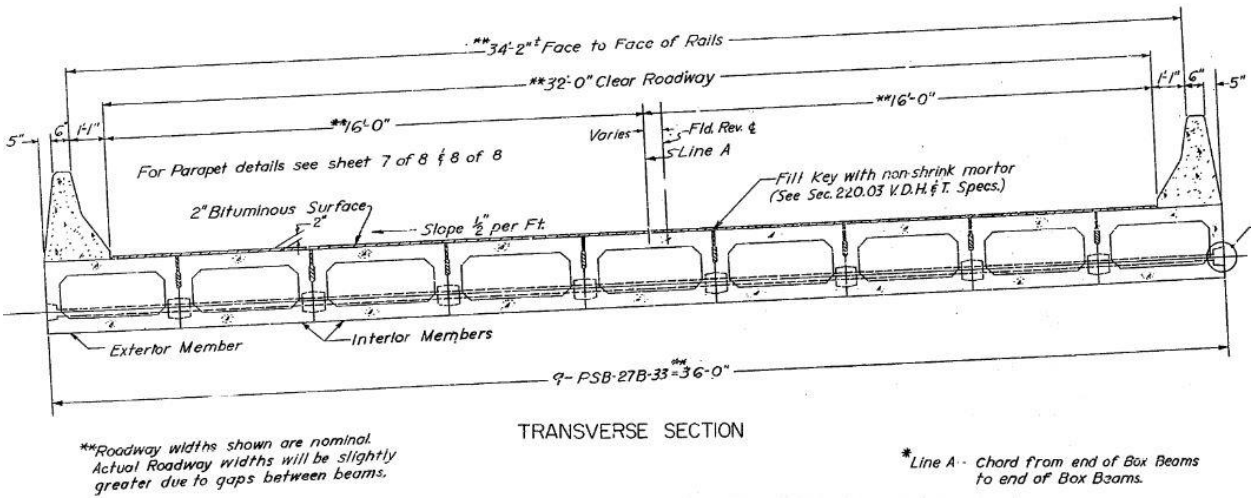

Figure 6. Transverse View of Buffalo Branch Bridge Plans

Adjacent Member Bridges

VDOT stipulates the design requirements for adjacent box beam bridges in Part 2 of the Manual of Structure and Bridge Division Volume V (VDOT, 2015). With the exception of freeways and urban/rural principal arterials, adjacent box beam bridges may be used on all other

roadway classifications, using a wearing surface according to the average daily traffic and average daily truck traffic, as shown in Table 1.

Table 1. Deck/Overlay Requirements for Adjacent Box Beam Bridges

Design Year ADT	ADTT	Deck/Overlay
≤4000	≤100	Asphalt Overlay
>4000	100 < ADTT ≤ 200	Concrete deck 5 in thick with single layer of reinforcement
>4000	>200	Concrete deck 7 ½ in thick with two layers of reinforcement

For adjacent box beams, less than 39 in deep, VDOT requires transverse post-tensioning strands at mid-depth of the beams to tie the precast members together prior to grouting. If the ends of the prestressed concrete box beams are constrained from lateral movement by wing haunches, the following tie layouts are required:

- for spans ≤ 30 ft: 1 tie at midspan
- for spans ≤ 60 ft: 2 ties at third points
- for spans > 60 ft: 3 ties at quarter points.

However, if the ends of the prestressed concrete box beams are not constrained from lateral movement, then the following tie layouts are required:

- for spans ≤ 30 ft: 3 ties at midspan and each end
- for spans ≤ 60 ft: 4 ties at third points and each end
- for spans > 60 ft: 5 ties at quarter points and each end.

The nine box beam sections in the Buffalo Branch Bridge were 4 ft wide; a typical cross-section is shown in Figure 7.

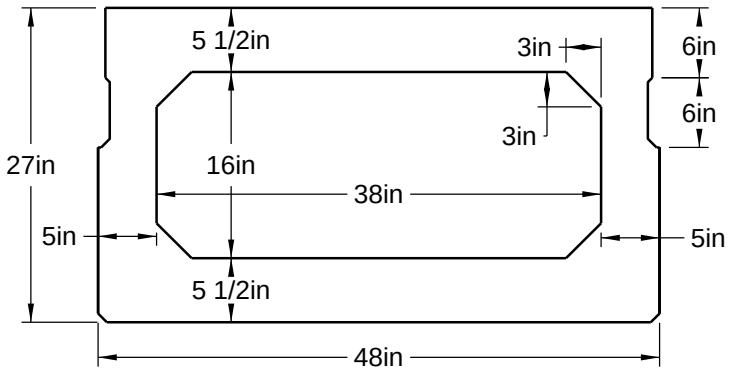

Figure 7. VDOT 4-ft-Wide Box Beam (VDOT, 2015)

The typical longitudinal connection that VDOT specifies is a partial depth shear key shown in Figure 8. Prior to placing the grout, the shear key is prepared by cleaning, sandblasting, and by creating a saturated surface dry (SSD) condition. This preparation has been shown to improve the bond between the grout and the precast member. VDOT outlines the waterproofing requirements for adjacent box beam bridges in Section 416 of the *Road and*

Bridge Specifications (VDOT, 2007). VDOT outlines different procedures using epoxy-resin compounds and aggregates and also a membrane and primer.

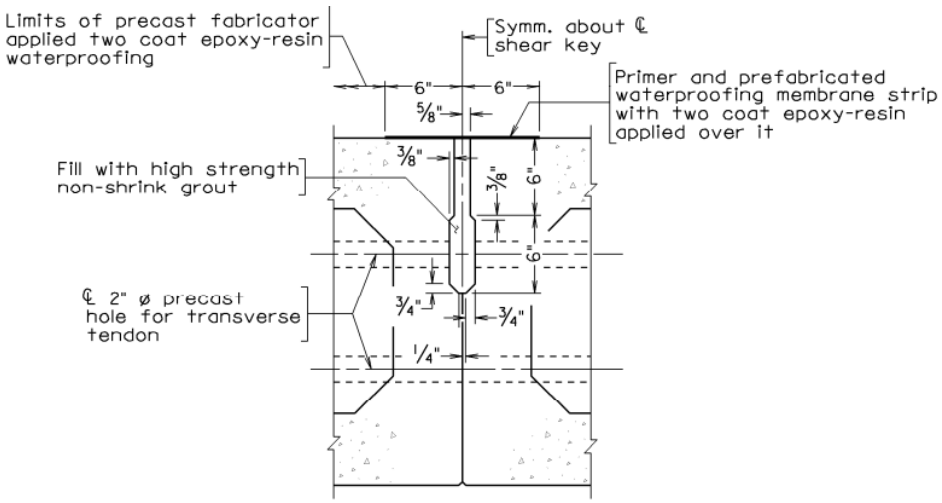

Figure 8. VDOT Shear Key Detail (VDOT, 2015)

Ultra High Performance Concrete (UHPC)

Graybeal (2014) recommended using UHPC for field-cast connections between precast bridge members in accelerated bridge construction because the material gains strength quickly and will not create weak points in the structure. Another advantage for using UHPC in connections is that the development length required for reinforcing steel is greatly reduced as compared to normal concrete. Also, because of the superplasticizer present in the mix, UHPC is able to flow efficiently in small, tight spaces and be self-consolidating while maintaining a low water-to-cementitious material ratio and high strength properties. However, UHPC is not as fluid as grout, which is the currently accepted material for precast member connections. According to Yuan and Graybeal (2014), field-cast UHPC connections had been used in 32 bridges in the United States, as of 2013.

Very High Performance Concrete (VHPC)

Research completed at the University of Nebraska by Akhnoukh (2008) aimed to develop a cost-efficient, non-proprietary high performance concrete. The methods explored to reduce costs were using locally available materials, eliminating the steel fibers, and replacing some of the cement with Class C fly ash. The average cost per cubic yard of the high performance mixes developed was $360. As fibers account for a majority of the mixture's cost, eliminating them was the greatest economic value. Akhnoukh tested 19 mixes in three stages.

Researchers at Virginia Tech continued Akhnoukh's work by modifying and testing one of Aknoukh's promising mixes, Mix 11, which had the highest 28-day compressive strength (unpublished data). The researchers modified this mix by adding 2% steel fibers by volume, replacing the Type III cement with Type I/II cement, replacing the Class C fly ash with Class F fly ash, and changing the name to Mix B. The original and modified mixes are displayed in Table 2.

Table 2. VHPC Mix Design Development, Mix 11 and Mix B

Material	Akhnoukh's Mix 11, lb/yd^3	Virginia Tech Mix B, lb/yd^3
Sand	1449	1450
¼ in limestone	616	621
Cement	1120 (Type III)	1121 (Type I/II)
Fly Ash	240 (Class C)	240 (Class F)
Silica Fume	240	240
HRWR	75	67.5
Water	240	319
w/c	0.189	0.20
Steel Fibers	0	265

The tensile strength of Mix B was then investigated using a modification of the American Association of State Highway and Transportation Official's (AASHTO) T 132-87 standard (2013), which ordinarily tests the tensile strength of hydraulic cement mortar. The mortar briquette test uses a 3-in-long x 1-in-thick dog bone-shaped specimen with a 1-in^2 cross-sectional area at mid-length. The dog bone is placed in self-aligning grips, which apply tension to the dog bone specimen while the load applied and the crosshead extension are recorded. The material properties of Mix B are shown in Table 3.

Table 3. Mix B Material Properties

Material Property	Age, days	Strength, psi
Compressive Strength	≈ 28	16800
Splitting Tensile Strength	≈ 28	2000
Mortar Briquet Test	>> 28	916

Other variations of Akhnoukh's Mix 11 were also created by changing the ratio of the cementitious materials and adding different quantities of slag; however Mix B was determined to have the best test results. Subsequently, Virginia Tech renamed Mix B as VHPC because the new material did not quite meet the strength requirements of UHPC but was still very strong and high-performing.

Lap Splices in UHPC and VHPC

Halbe et al. (2015) reported on tests to determine the minimum lap splice length required to fully develop No. 4 bars in UHPC and VHPC. Transverse tensile stresses can develop at the connections between adjacent members due to traffic loads, shrinkage and temperature. The proposed connection required a drop-in splice bar to carry this tension force in combination with UHPC or VHPC. Therefore, the required splice length needed to be determined. A test method was developed to mimic the lap splice region in adjacent precast members, and splice lengths of 3 in to 6 in were tested.

In the tests, the tension reinforcement in all of the specimens exceeded the yield stress of 60 ksi; therefore, a 3-in lap splice distance was determined to be adequate to yield the steel.

However, due to ductility concerns, the recommended lap splice length for a No. 4 reinforcing bar in UHPC or VHPC was 5 in.

Summary of Background

The service life of adjacent box beam and adjacent voided slab bridges is often limited by premature deterioration of the shear key in the longitudinal beam-to-beam joint. To save money and time, rehabilitating existing bridges is more advantageous than replacement. The high performance of VHPC makes the material a suitable option to replace conventional grout in the shear keys. Also, VHPC is a lower-cost alternative to UHPC, yet has similar material properties. The new rehabilitation plan requires cutting pockets across the joints, into which a short piece of reinforcing steel is placed and then filled with VHPC along with the rest of the shear key. The smaller lap splice distance required to develop the reinforcing steel is another advantage to using VHPC instead of grout as the shear key material.

PURPOSE AND SCOPE

Due to the problems that arise when reflective cracking appears, the purpose of this project was to continue the work presented in Halbe (2014) and develop an improved rehabilitation method for adjacent box beam and voided slab bridges and implement the new retrofit method on the Buffalo Branch Bridge near Staunton, Virginia. The goal of the improved connection was to increase the service life of the bridge well beyond that obtained by simply replacing the deteriorated shear key with an identical shear key design.

To accomplish these objectives, the following tasks were completed:

1. Additional material testing of the VHPC mixture was performed to confirm that the material was a viable long-term replacement for the UHPC.

2. Cyclic load tests were performed on a connection similar to those tested by Halbe, but with no direct splice to a reinforcing bar in the box beam.

3. Live load tests on the Buffalo Branch Bridge were conducted to characterize the pre-repair and post-repair condition.

4. The researchers worked with the contractor to implement the new connection detail on the Buffalo Branch Bridge and documented the process.

Based on the work completed in this research program, the efficacy of the repair was evaluated and recommendations have been made for future implementation of the repair technique.

METHODS

This section explains the details of the tests performed for this project. The first section explains the material tests executed. The second section presents the connection testing similar to that used in the research done by Joyce (2014) to develop a more durable connection in adjacent voided slab bridges. The third section outlines the pre-repair and post-repair live load tests of the Buffalo Branch Bridge. The last section presents the rehabilitation method used on the bridge.

Material Property Testing

Material Mix Designs and Mixing Procedures

Material tests were performed on five different mix designs. The mix designs for one cubic yard of each material tested and the mixing procedures are outlined here.

UHPC

UHPC was made using the proprietary premix Ductal. Ductal is a high strength, fiber reinforced, self-consolidating concrete. The mix design is presented in Table 4.

Table 4. UHPC Mix Design

Constituent	lb/yd^3
Ductal Premix	3700
Water	219
Premia 150 (Superplasticizer)	51
½-in Steel Fibers (2% by volume)	263
w/cm	0.06

The mixing procedure for UHPC was precisely outlined by the manufacturer and followed. To begin, the mixer needed to be dry, not damp. The Ductal Premix was added and mixed for two minutes to disperse any large pack-set clumps. Next, the water and Premia 150 Superplasticizer were added and mixed for one minute until the mix was wet and had the consistency of bread dough. The mixer was then stopped and quickly scraped. Afterwards, mixing continued until the mix was flowable and no material was sticking to the sides of the mixer, which typically took about three minutes. Fibers were then added, preferably not clumped together, with the mixer continuing for another four minutes until the fibers were evenly distributed. The total mix time was approximately ten minutes.

VHPC

VHPC with large aggregate (named VHPC-Large), created at the University of Nebraska and modified at Virginia Tech as a high strength, fiber reinforced, self-consolidating concrete, is a more economical option than UHPC because of the addition of coarse aggregate and because of the non-proprietary development. The mix design is outlined in Table 5, and is essentially the

same as Mix B presented in Table 2, but with the high range water reducer (HRWR) dosed in ounces per hundred pounds of cementitious materials (oz/cwt) instead of lb/cwt. Note that a range is given for HRWR because the amount varied with each batch depending on the amount required to attain the desired workability.

Table 5. VHPC-Large Mix Design

Constituent	lb/yd^3
Water	319
Cement	1121
Fly Ash	240
Silica Fume	240
Sand	1450
¼-in Limestone	621
1.2 in Steel Fibers (2% by volume)	265
HRWR	22-26 oz/cwt
w/cm	0.20

VHPC-Large was developed with ¼-in aggregate and 1.2-in long steel fibers and was intended to be used in closure pours. However, when trying to use VHPC in the connections of adjacent member bridges with only a ¾ in gap at the top of the keyway, it was determined that the aggregate and fibers originally selected were too large to fit in the narrow shear keys. Due to this size restriction, a second VHPC mix was designed with 1/8-in aggregate and ½-in-long steel fibers. The mix with the smaller aggregate and fibers was named VHPC-Small, and the mix design is shown in Table 6.

Table 6. VHPC-Small Mix Design

Constituent	lb/yd^3
Water	319
Cement	1121
Fly Ash	240
Silica Fume	240
Sand	1345
⅛-in Limestone	660
½-in Steel Fibers (2% by volume)	260
HRWR	22-26 oz/cwt
w/cm	0.20

Both VHPC mixes were mixed using the same procedure. Initially, the mixer was sprayed down to be damp. The coarse and fine aggregate and half the water were added and mixed for five minutes until damp. The mixer was then scraped and continued mixing for another two minutes. The cement, fly ash, silica fume, and remaining water were then added and mixed for five minutes before scraping the sides of the mixer again. The HRWR was then added slowly and mixed for three minutes in order to obtain the desired consistency. Finally, the fibers

were added and mixed for two minutes before placing. The total mix time was approximately seventeen minutes.

Deck Concrete

VDOT Class A4 modified concrete is a standard Virginia bridge deck concrete. This mix design was chosen so that the durability test results could be compared to a more comprehensive group of data. The mix design is shown in Table 7.

Table 7. A4 Deck Concrete Mix Design

Constituent	lb/yd^3
Water	286
Cement	635
Fine Aggregate	1286
Coarse Aggregate (# 57 Stone)	1734
AEA	141 mL
HRWR	1880 mL
Retarder	564 mL
w/cm	0.45

The mixing procedure for the A4 deck concrete mix was similar to the VHPC mixes. Initially, the mixer was dampened and the fine and coarse aggregate and half the water were added and mixed until damp. The cement and remaining water were then added and mixed. Finally the air entraining admixture (AEA), HRWR, and retarder were added and mixed until the concrete reached a slump of 2 in to 4 in and the air content was between 5% and 8% as per VDOT specifications.

Grout

Quikrete's non-shrink precision grout was chosen because the material met the requirements for ASTM C1107, as required by the VDOT *Road and Bridge Specifications* (VDOT, 2007). The mix design is shown in Table 8. The amount of water added was based on the grout being flowable. The mixer was dampened and the bagged grout mix and water were added. After about five minutes, the grout was ready to be placed.

Table 8. Grout Mix Design

Constituent	lb/yd^3
Water	23
Premix Quikrete's Non-Shrink Precision Grout	111

Material Property Characterization Tests

Table 9 presents an overview of the tests done on the materials.

Table 9. Material Tests Overview

Test	Specimen	Material	ASTM Standard	Reference
Compressive Strength	4 in x 8 in Cylinders	UHPC, VHPC-Small VHPC-Large, A4 Deck Concrete, Grout	C39	ASTM (2014a)
Compressive Strength	2 in Cubes	VHPC-Small	C109	ASTM (2013)
Splitting Tensile Strength	4 in x 8 in Cylinders	UHPC, VHPC-Small VHPC-Large, A4 Deck Concrete, Grout	C496	ASTM (2011)
Modulus of Elasticity	4 in x 8 in Cylinders	UHPC, VHPC-Small VHPC-Large, A4 Deck Concrete, Grout	C469	ASTM (2014b)
Bond with Rebar	6 in x 6 in x 12 in Blocks	VHPC-Small and VHPC-Large	N/A	Johnson (2010)
Bond with Concrete	2 in x 1 in Pucks	VHPC-Small, VHPC-Large, and Grout	D7234	ASTM (2012b) and Scholz et al. (2007)
Workability	N/A	VHPC-Small and VHPC-Large	C1611	ASTM (2014c)
Durability	3 in x 4 in x 16 in Bars	UHPC, VHPC-Small VHPC-Large, A4 Deck Concrete, Grout	C666	ASTM (2008)
Free Shrinkage	3 in x 3 in x 11¼in Bars	UHPC, VHPC-Small VHPC-Large, A4 Deck Concrete	C157	ASTM (2014d)
Free Shrinkage	3 in x 3 in x 12 in Bars	A4 Deck Concrete, Grout	N/A	N/A

Compressive Strength

Compressive strength tests were performed in accordance with ASTM C39 (2014a) with 4 in x 8 in cylinders. The cylinders were cured by placing 4-mil plastic over the top to ensure that the moisture did not escape. On the day of testing, UHPC and VHPC cylinders were typically saw-cut to obtain a uniform loading surface. The ends were either capped in sulfur or with neoprene end caps for loading. Cylinders were typically tested in groups of three and at ages ranging from 12 hr to 28 days. The compressive strength of the UHPC and VHPC-Small mixtures were also tested in accordance with ASTM C109 (2013) using 2-in cubes.

Splitting Tensile Strength

Tensile strength was measured using the procedure outlined in ASTM C496 (2011) with 4 in x 8 in cylinders. The UHPC and VHPC cylinders were cured and saw-cut in the same fashion as the compressive cylinders, but they were not capped. The cylinders were placed between thin bearing strips made of plywood in a jig for aligning the concrete cylinder and loaded to failure. Cylinders were typically tested in pairs at ages ranging from 12 hr to 28 days.

Modulus of Elasticity

Cylinders used for compressive strength tests were also used to determine the modulus of elasticity in accordance with ASTM C469 (2014b). A modulus collar was attached to the cylinders and the cylinders were loaded within the prescribed range of rate while recording the gauge readings and load.

Reinforcing Steel Bond

A modified version of the pull out tests presented in Johnson (2010) was performed to determine the bond of the VHPC mixes with reinforcing steel. The tests performed in this study were simplified with slightly smaller blocks and No. 4 reinforcing steel embedded at the center of the blocks, as the only objective was to measure if the reinforcing steel slipped out of the concrete or yielded. To prevent the reinforcing steel from pulling out the top section of the block in a cone failure, the top of the reinforcing steel was debonded using PVC pipe in the bottom 4 in and top 3 in of the block, leaving 5 in of the reinforcement bonded in the middle of the concrete block, as shown in Figure 9.

Figure 9. Bonded versus Debonded Reinforcing Steel for Pull Out Specimen

Several pull out specimens were cast at the same time so that the tests could be performed at different early ages. The instrumentation for the pull out tests consisted of linear variable differential transformers (LVDTs) and wire pots for measuring displacement. The bottom LVDT was used to determine if the reinforcing steel was slipping through the VHPC and being pulled out the top by a center-hole ram. The top LVDT and the wire pot were both attached to the top of the ram to measure how far the steel had been elongated. A load cell was used to determine the load that was applied by the ram and the rate at which the load was applied. Because the ram was manually controlled, the approximate load rate ranged from 100 lb/sec to 500 lb/sec. The test set-up and instrumentation are shown in Figure 10. The pull out specimens were tested 12 hr, 1 day, 2 days, and 7 days after placing.

Bond with Concrete

To quantify the bond strength of the VHPC with the precast concrete members, a modified version of ASTM D7234 (2012b) was performed, as shown in Figure 11. The standard test requires a continuous layer of coating on a concrete substrate. Cuts are then made through both the coating and concrete substrate to attach the loading fixture. The loading fixture is then pulled with a tensile force normal to the test surface.

The modified tests were conducted by casting 2 in diameter x 1 in tall pucks of VHPC directly on the bottom of precast concrete members used in a previous project. One advantage to making individual pucks instead of casting a continuous surface is that effects of surface

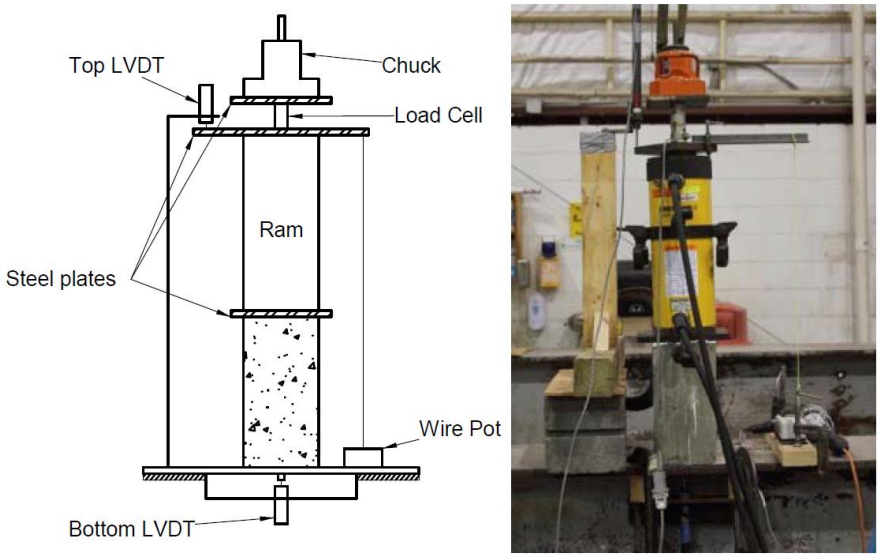

(a) **(b)**

Figure 10. (a) Schematic and (b) Photo of Pull Out Test Setup

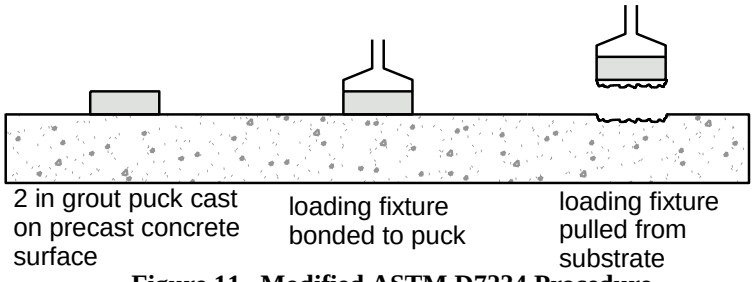

Figure 11. Modified ASTM D7234 Procedure

preparation could also be assessed, such as sand blasting and surface dryness. The bottom of the precast member offered a large surface area for many pucks to be cast, yet had the same smooth surface as the shear key due to metal formwork. The pucks were cast on a horizontal surface because it was not practical to cast them vertically. These test results were compared to specimens tested by Joyce (2014), which were cast in an identical manner. An overview of multiple VHPC pucks being cast on the bottom of a precast member is shown in Figure 12.

Ordinarily, a skin-like layer starts to form at the surface of VHPC immediately after being placed. In order to epoxy a threaded metal cap used to apply the tensile force, a piece of duct-tape covered wood was set on the surface of the puck to prevent the skin-like layer from forming on the surface. A threaded metal cap was typically epoxied to the top of the pucks 12 to 24 hours before testing and is also shown in Figure 13. A hook was screwed into the metal cap and attached to a tension load cell, with load being applied by twisting a load jack. The test set-up is shown in Figure 14.

Workability and Flow

One way of quantifying workability is in accordance with ASTM C1611 (2014c), as shown in Figure 15. In this research, the spread was measured at different times during the mixing procedure to investigate how rapidly the flow changes.

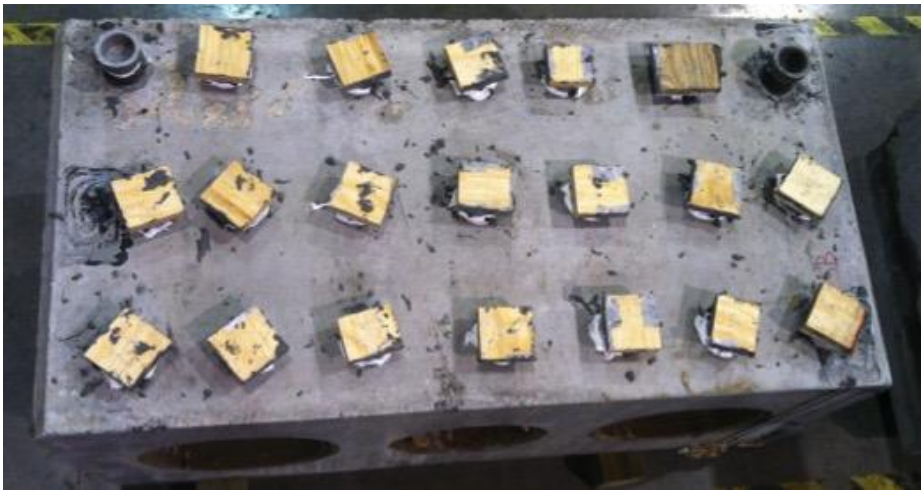

Figure 12. Bond Test Specimens

(a) **(b)**

Figure 13. (a) Bond Puck with Wood Top and (b) Bond Puck with Hook Attached

Figure 14. Bond Test

Figure 15. Inverted Cone Slump Testing

In addition, the flow was measured using unconventional methods to simulate field conditions. A 6 in x 6 in x 5 ft box test was built to mimic a closure pour and determine the distance the VHPC-Large could reasonably be expected to flow. After placing six large scoops of the VHPC-Large into one end of the box, the researchers recorded the distance the material had flowed after 15 sec. The test setup is shown in Figure 16.

Figure 16. Box Test

The shear key slope flow test was designed to replicate the depth and slope of the shear keys along the length of the Buffalo Branch Bridge to determine if the shear key at the low end of the bridge would need to be covered to prevent the VHPC-Small from overflowing. A 1.5 in x 12 in x 8 ft box was made and initially placed on supports at the same 0.8% grade slope as the bridge. The VHPC-Small was placed in the top of the slot starting at the low end and moving to the high end. Because the VHPC-Small did not overflow on the low end after 5 min with continued tapping on the sides to agitate it, the elevation difference was changed to 5 in to represent the full elevation change of the bridge. This resulted in a 5% slope for the box. The shear key slope flow test is show in Figure 17.

Figure 17. Shear Key Flow Test

The transverse slope of the bridge was also replicated by creating formwork for the geometric cutouts recommended to be used in the Buffalo Branch Bridge rehabilitation, as discussed in the section *Implementation of the Repair Method on Buffalo Branch Bridge*. Both a dog bone- and a bowtie-shaped shear key were made and are shown in Figure 18.

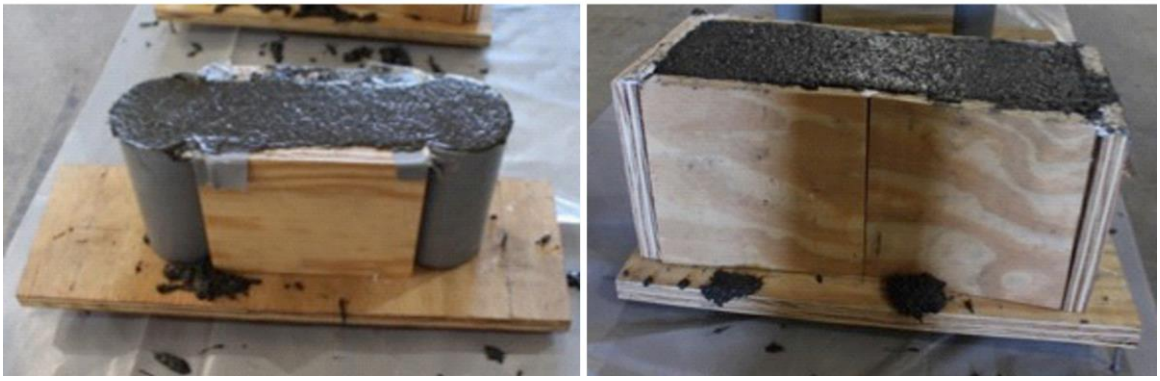

(a) **(b)**

Figure 18. (a) Dog Bone and (b) Bowtie Flow Test Setup

Shrinkage

Shrinkage tests were performed in accordance with ASTM C15 (2014d). Prisms (3 in x 3 in x 11¼ in) were cast in pairs and the shrinkage was typically measured daily for the first 14 days after demolding. Measurements were then taken weekly until 50 days when the measurements were taken monthly.

The ASTM C157 comparator to measure length change had a very small tolerance on acceptable lengths. Three of the shrinkage specimens cast were out of that range and were not able to be measured. These bars were instrumented with locating discs for a DEMEC extensometer on the top and bottom of the specimen to measure the surface shrinkage. Measurements were taken at the same time interval as the rest of the shrinkage prisms.

Durability

Durability was measured in accordance with ASTM C666, Procedure A. Three freeze/thaw specimens 3 in x 4 in x 16 in were cast for each of the five mixes. Typically, the specimens were measured for weight and resonant frequencies every 35 cycles. Data was recorded from 0 cycles to 306 cycles when the freeze/thaw machine would no longer cycle temperatures. The freeze/thaw machine exhibited problems maintaining a constant freezing and thawing rate.

Cyclic Tests of Non-Contact Lap Splice Connection

Halbe (2014) and Joyce (2014) worked to develop durable adjacent member shear key details for new construction using blockouts that exposed part of a transverse bar in adjacent members, which could be tied together by a splice bar across the longitudinal joint (as suggested in Figure 4). At the conclusion of Joyce's work, there was one extra sub-assemblage of voided slab sections remaining and this specimen was used to investigate the non-contact lap splice connection. The specimen was modified by cutting the exposed transverse bars and placing a short piece of reinforcing steel in the otherwise empty blockout. This created a non-contact lap splice between the drop in bar and the nearest stirrup approximately 4 in away, while otherwise maintaining the conventional shear key. This modification represented the detail to be used in the retrofit of an existing structure designed with adjacent box beams. A schematic of the sub-assemblage and test set-up is shown in Figure 19. The joint and shear key were filled with VHPC-Large. The connection pocket can be seen in Figure 20 with a non-contact splice bar in place.

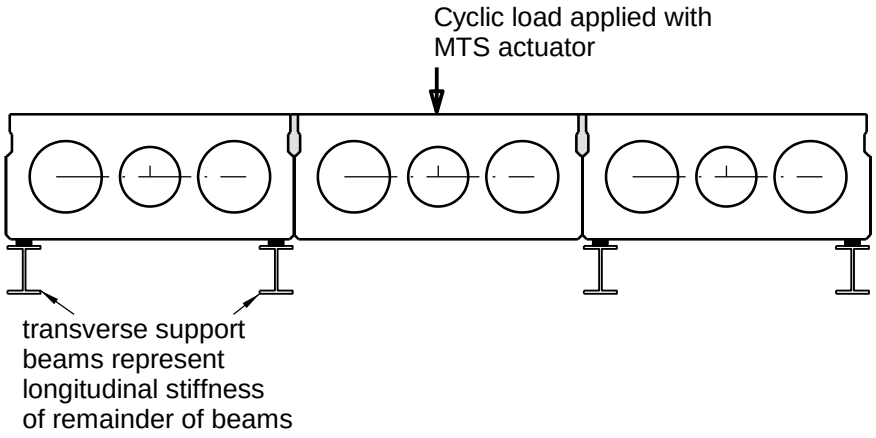

Figure 19. Sub-Assemblage Test Setup

Figure 20. Non-Contact Voided Slab Connection

Joyce's finite element modeling of both a representative voided slab bridge and the sub-assemblage helped to determine that the transverse tensile stresses in the shear keys of the bridge system subjected to an AASHTO design truck loading could be replicated by imposing a vertical displacement of 0.03 in on the sub-assembly specimen supported by W8x15 beams. The sub-assemblage was instrumented with LVDTs at the bottom of the shear keys on both sides of each joint, which can be seen in Figure 21. The purpose of the LVDTs was to monitor the joint opening during the testing.

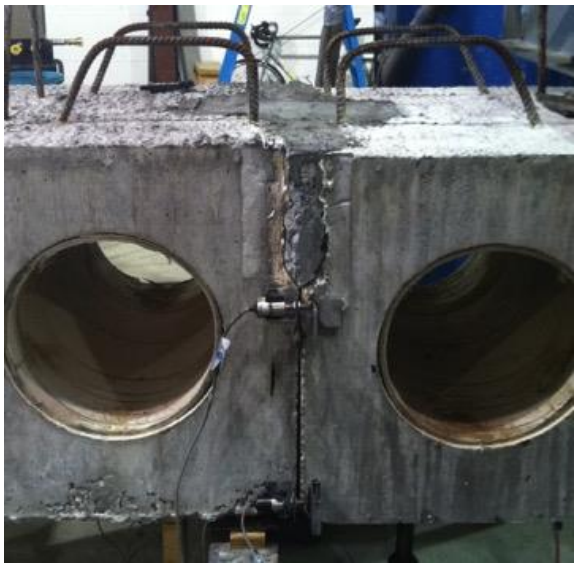

Figure 21. Joint Instrumentation

Testing began with an initial static test in which the center voided slab was lowered to a vertical displacement of 0.03 in and then raised back up by 0.03 in so that the specimen returned to its initial "zero point." After the initial static test, cyclic tests began by lowering the specimen by 0.015 in and then cycling the deflection between 0.03 in and the "zero point" at a frequency of 3 hertz. Static tests were performed after each group of cycles, with the groups being 10, 100, 1,000, 10,000 cycles, and then every 100,000 cycles until the test reached 1,000,000 cycles.

During the cyclical testing, water was ponded on top of the joints to monitor if cracking was occurring. The final static test after 1,000,000 cycles was an attempt to completely fail the specimen.

Buffalo Branch Bridge Pre- and Post-Repair Live Load Tests

Instrumentation

Sensors were used to record the data that was most pertinent, which included vertical deflections and longitudinal strains of individual box beams, and the relative vertical and horizontal joint movements between adjacent members. The instrumentation described in this section was almost identical for the pre-repair test and the post-repair test, with slight differences explained as necessary.

Strain Transducers

Strains were recorded at the midspan of each box beam using Bridge Diagnostics, Inc. (BDI) strain transducers. These gauges comprise four strain gauges in a full Wheatstone bridge configuration and calibration factors are provided by BDI for each transducer. The metal feet on the bottom of the BDI strain transducers were glued to the bottom of the box beam members, as shown in Figure 22. Note that these gauges were oriented in-line with the box beams in order to measure the longitudinal strain of the members. Therefore, the transducers were not perpendicular to the line in the figure, which was along the bridge skew at midspan.

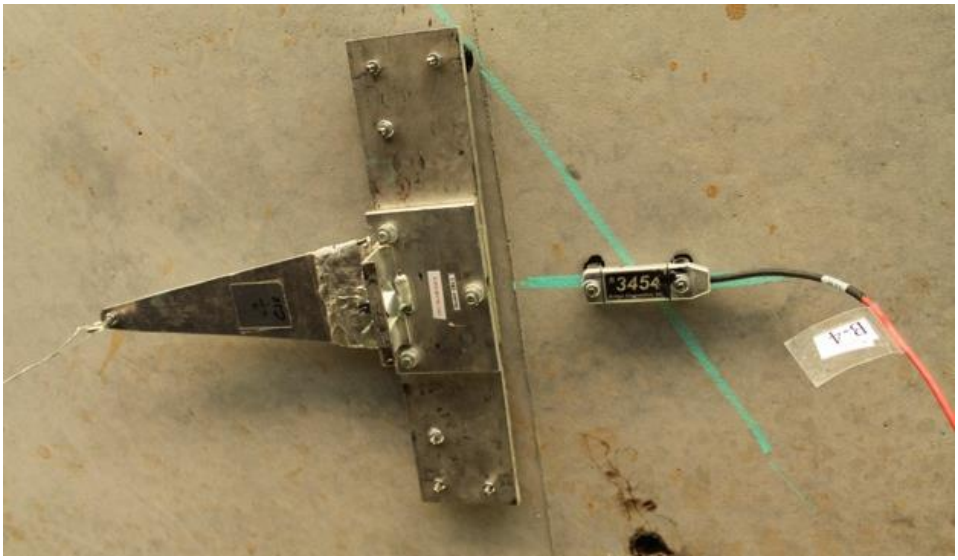

Figure 22. BDI and Deflectometer

Deflectometers

Deflections were measured using home-made deflectometers shown in Figure 22. The deflectometers consisted of a flexible aluminum plate with four strain gauges in a full bridge configuration sandwiched between two rigid aluminum plates to create a cantilever. To measure

the deflection, the deflectometers were calibrated in the lab by correlating recorded strain values with known deflections of the end of the cantilever. In the field, the deflectometers were attached to the bridge by gluing the metal feet to the box beam members. The end of the deflectometer cantilever was pre-deflected using a high-strength wire tied down to a concrete cylinder sitting on the ground, as shown in Figure 23. In this way, when a truck load was applied and the bridge deflected, the deflection of the cantilever tip was reduced, which reduced the strain recorded by the gauges.

Figure 23. Concrete Cylinders Weighing Down Wires Used for Pre-deflection

Linear Variable Differential Transformers (LVDTs)

LVDTs were used to measure the horizontal and vertical relative displacements of adjacent box beam members, and were strategically placed at the location of the highest expected relative girder displacements. The horizontal LVDT was glued to the bottom edge of a box beam and a wooden block was glued to the bottom edge of the neighboring box beam so that the LVDT measured differential horizontal movement between the two box girders. Likewise, the vertical LVDT attachment was glued to the bottom edge of a box beam and a piece of steel was glued to the bottom edge of the neighboring box beam such that the vertical LVDT was in contact with the plate at the center of the joint. See Figures 24 and 25 for the horizontal and vertical measurements setups, respectively.

Figure 24. Horizontal LVDT

Figure 25. Vertical LVDT

Glue and Accelerant

Loctite 410 glue and Loctite 7452 accelerant were used to attach all sensors onto the bottom of the box beam members. The glue and accelerant system took seconds to cure.

Instrumentation Layout

BDI strain transducers and deflectometers were placed at midspan on the bottom of each box beam. Vertical and horizontal LVDTs were placed at midspan and quarterspan on the two external downstream joints, where the most leaking appeared to have occurred. The same was done for the two external upstream joints in order to compare the results of the relative displacement in deteriorated joints with seemingly undamaged joints. The instrumentation plan for the pre-repair and post-repair tests are shown in Figure 26 and Figure 27, respectively. The only difference is that the relative displacements of the joints at the quarter points were not measured in the post-repair tests, because results were negligible in the pre-repair tests.

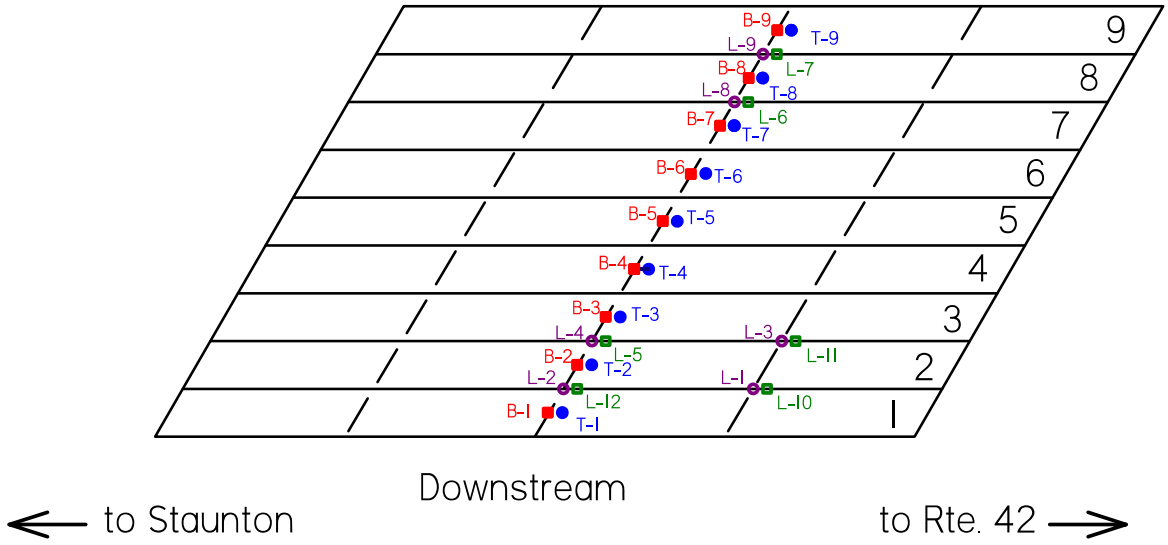

Figure 26. Instrumentation Plan for Pre-Repair Test
(T = Deflectometer, B = Strain Gage, and L = LVDT)

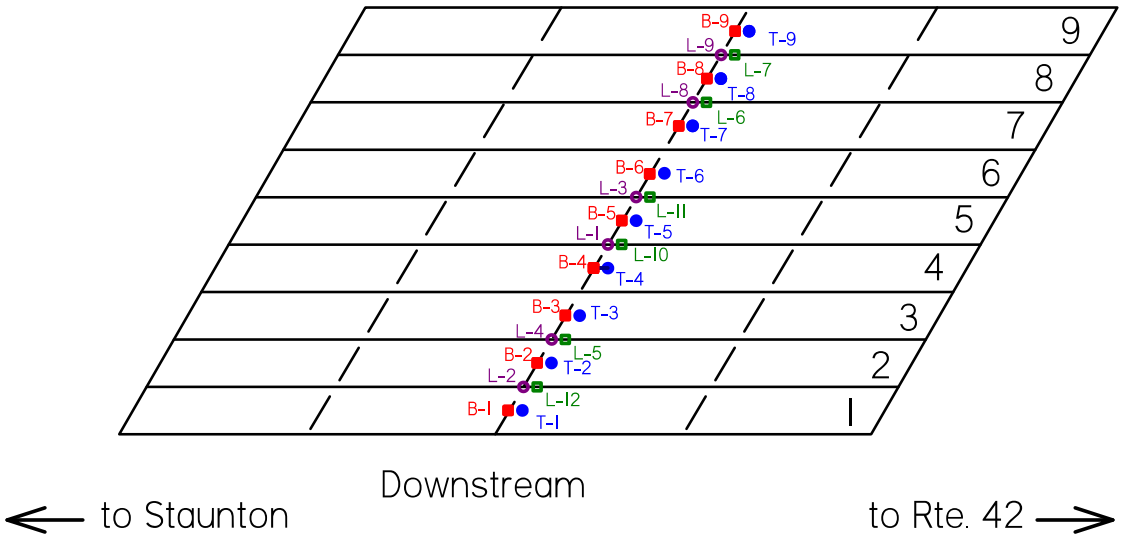

Figure 27. Instrumentation Plan for Post-Repair Test (T = Deflectometer, B = Strain Gage, and L = LVDT)

Data Acquisition

The data acquisition system (DAS) and software used was the Structural Testing System (STS) by BDI. The STS consisted of three main components: the computer software, DAS base station, and nodes. The sensors were wired directly to the nodes, shown in Figure 28. Each node was capable of connecting to four sensors. The BDI nodes transmitted the data wirelessly to the computer through the DAS base station.

Loading Procedure

A total of six quasi-static load cases were tested, each in three separate runs. Brightly colored chalk lines were drawn on the bridge deck at the joints, marking the outside edge of the front left tire of the load truck(s), which traversed the bridge at the slowest possible speed of two to three mph, as shown in Figure 29.

Figure 28. BDI Nodes

Figure 29. Marking Location of Truck(s)

Trucks

The load for each test was provided by two VDOT dump trucks loaded to approximately 25 tons each. The measured axle loads for each truck are shown in Figure 30 and Figure 31. The loading trucks had similar dimensions and are shown in Figure 32 and Figure 33. The width of each of the rear tires was 1 ft, therefore the overall width of the truck was approximately 8 ft.

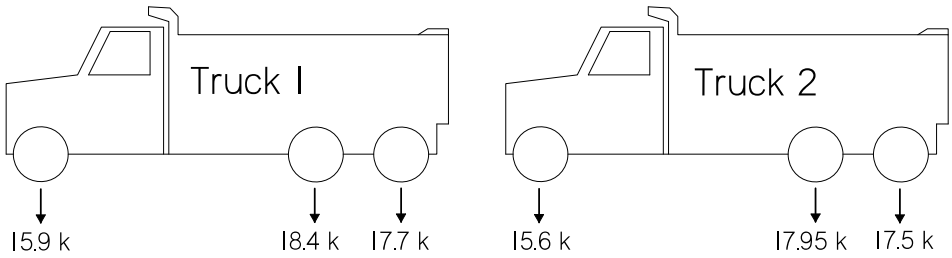

Figure 30. Axle Weights of Loading Trucks for Pre-Repair Tests

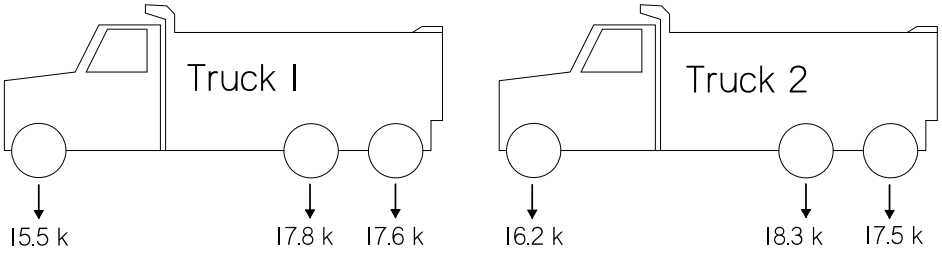

Figure 31. Axle Weights of Loading Trucks for Post-Repair Tests

Load Cases

As previously mentioned, the two exterior downstream joints, Joint 1 (between beams 1 and 2), and Joint 2 (between Beams 2 and 3), showed the most signs of deterioration. Therefore, Load Case 1 (shown in Figure 34) and Load Case 2 (shown in Figure 35) were chosen to cause the largest relative joint displacements at those two joints. Load Case 3, shown in Figure 36, was chosen to obtain the maximum midspan deflections and longitudinal strains in the downstream beams.

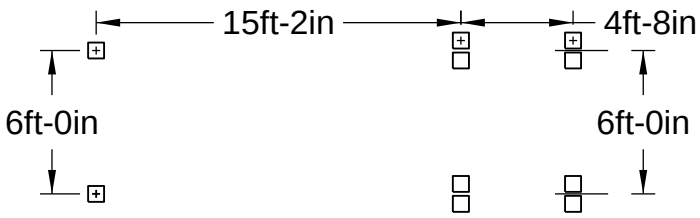

Figure 32. Dimensions of Loading Trucks for Pre-Repair Tests

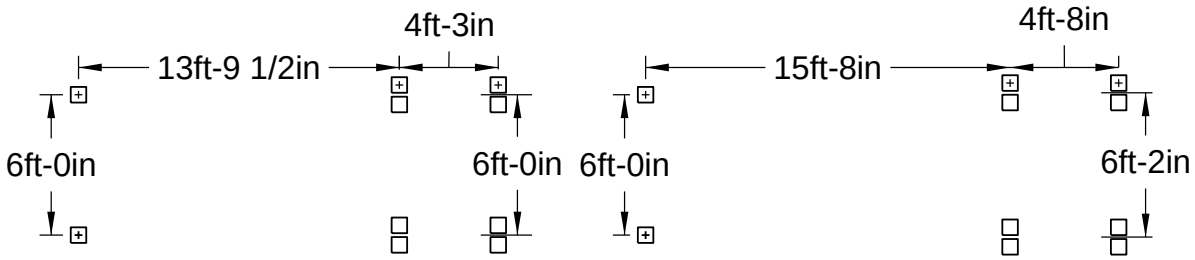

Figure 33. Dimensions of Loading Trucks for Post-Repair Tests

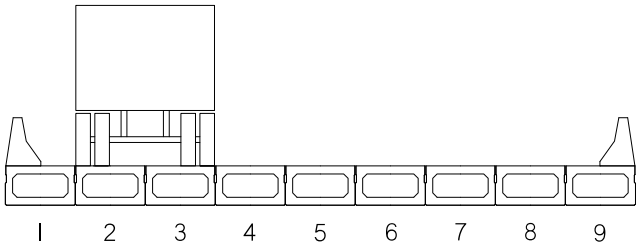

Figure 34. Load Case 1

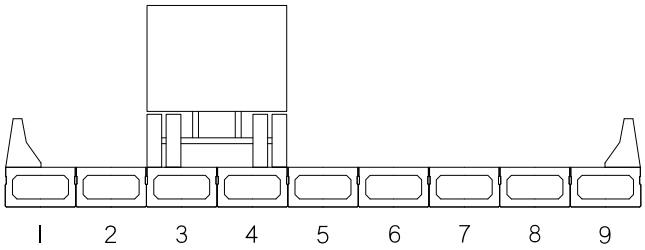

Figure 35. Load Case 2

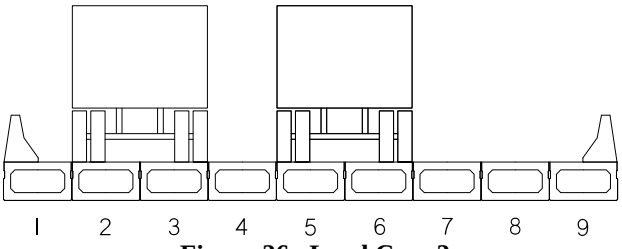

Figure 36. Load Case 3

Load Cases 4 through 6 mirrored the first three load cases on the upstream side of the bridge in an attempt to gather the same information for joints that had been deemed to be in relatively good condition. Load Cases 4 through 6 are shown in Figures 37 through 39, respectively.

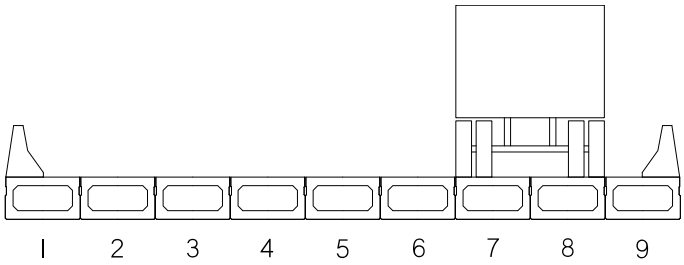

Figure 37. Load Case 4

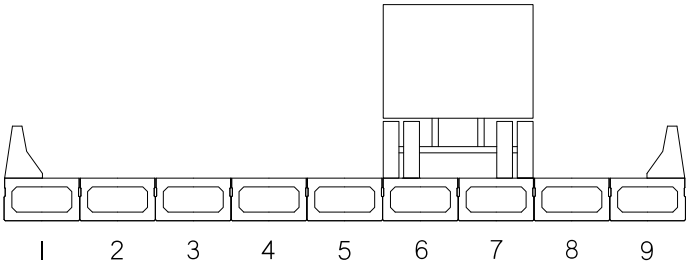

Figure 38. Load Case 5

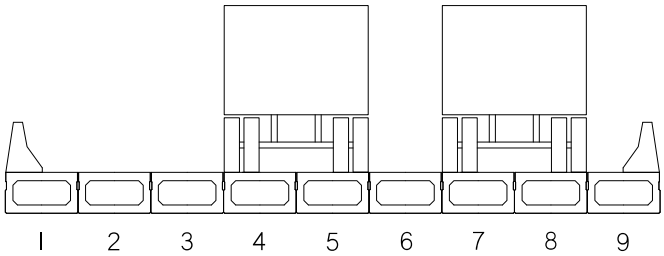

Figure 39. Load Case 6

Live Load Distribution Factors

Live load distribution factors (LLDFs) determine the fraction of load that each individual girder is designed to carry. According to Collins (2010), LLDFs are influenced by the system stiffness, topping conditions, skew, and deterioration of joints. Two methods for calculating the LLDFs of the Buffalo Branch Bridge are presented. The first method is outlined in the AASHTO LRFD Bridge Design Specifications (2012); the second is presented by Collins (2010) to calculate the LLDFs based on test results for midspan vertical deflection and longitudinal strain.

According to AASHTO, the Buffalo Branch Bridge was classified as a type (g) cross-section shown in Figure 40. Type (g) includes precast solid, voided or cellular concrete box beams with shear keys and an integral concrete deck, but may or may not have transverse post-tensioning.

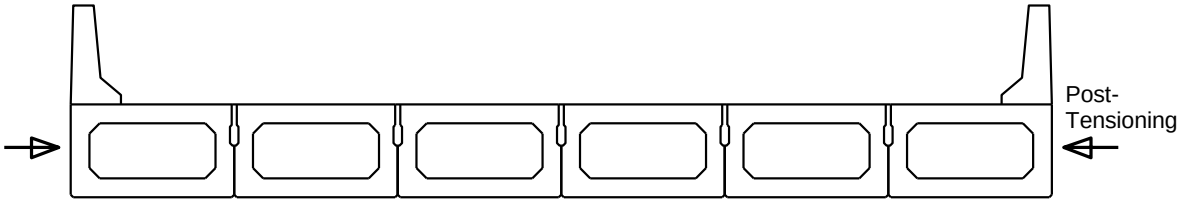

Figure 40. AASHTO Type (g) Cross-Section

The following equations associated with type (g) cross-sections were used to calculate the LLDFs for moments in interior beams:

One design lane loaded:

$$GDF = k\left(\frac{b}{33.3L}\right)^{0.5}\left(\frac{I}{J}\right)^{0.25} \quad \text{(Eq. 1)}$$

$$k = 2.5(N_b)^{-0.2} \geq 1.5 \quad \text{(Eq. 2)}$$

where

N_b = the number of girders
b = the girder width (in)
L = the span length (ft)
I = the moment of inertia (in^4)
J = the St. Venant torsional inertia (in^4).

Two or more design lanes loaded:

$$GDF_{interior} = k\left(\frac{b}{305}\right)^{0.5}\left(\frac{b}{12.0L}\right)^{0.2}\left(\frac{I}{J}\right)^{0.06} \quad \text{(Eq. 3)}$$

The range of applicability of Equations 1 through 3 is:

$$35 \leq b \leq 60 \quad \text{(Eq. 4)}$$

$$20 \leq L \leq 120 \quad \text{(Eq. 5)}$$

$$5 \leq N_b \leq 20 \quad \text{(Eq. 6)}$$

To calculate the LLDFs for moments in the exterior beams, the following equations were used:

$$LLDF = eLLDF_{interior} \quad \text{(Eq. 7)}$$

where for one design lane loaded:

$$e = 1.125 + \frac{d_e}{30} \geq 1.0 \quad \text{(Eq. 8)}$$

and for two design lanes loaded:

$$e = 1.04 + \frac{d_e}{25} \geq 1.0 \quad \text{(Eq. 9)}$$

where d_e is the horizontal distance from the centerline of the exterior web of exterior beam at deck level to the interior edge of curb or traffic barrier in feet.

The range of applicability of Equations 8 and 9 is:

$$d_e \leq 2.0 \quad \text{(Eq. 10)}$$

Due to the 30° skew of the Buffalo Branch Bridge, the LLDFs were reduced using the reduction factor, *r*:

$$r = 1.05 - 0.25 \tan(\theta) \leq 1.0 \quad \text{(Eq. 11)}$$

where θ is the angle of skew, in degrees. The range of applicability of Equation 11 is:

$$0° \leq \theta \leq 60° \quad \text{(Eq. 12)}$$

If θ is greater than 60°, the use θ = 60.

The second method, outlined in Collins (2010), was used to calculate the LLDFs using the midspan vertical deflections and longitudinal strains obtained from the live load tests. The following equation was used:

$$GDF = \frac{R_{max} n}{\sum_{j=1}^{m} R_{peak_j}} \quad \text{(Eq. 13)}$$

where

R_{max} = the maximum response of the girder
n = the number of trucks applying the load
m = the number of girders
R_{peak_j} = the maximum response of the j^{th} girder.

To account for the skew of the bridge, the sum of the maximum responses of all of the girders was used in the denominator.

Both methods were used to determine the LLDFs of the Buffalo Branch Bridge. The methods were used to compare distribution of loads before and after repairs.

Implementation of the Repair Method on Buffalo Branch Bridge

The rehabilitation plan for the Buffalo Branch Bridge is shown in Figure 41. The plan was for all of the joints to be completely cleaned out. The four interior joints were to be replaced with fresh grout and a Kevlar and epoxy topping. The four exterior joints were to be replaced with VHPC, with the half of span length nearest the obtuse skew corners also having geometric cutouts for the non-contact splice bars. The spacing for these cutouts was either 2 or 3 ft in order to assess how close the splices needed to be. Figure 42(a) shows the dimensions for the dog bone cutouts to be used in the upstream joints. Figure 42(b) shows the dimensions for the bowtie cutouts to be used in the downstream joints. Laboratory testing was performed on a variety of

cutout shapes and the dog bone and bowtie were determined to be the two best alternatives. The depth of the cutouts was to be 4 in.

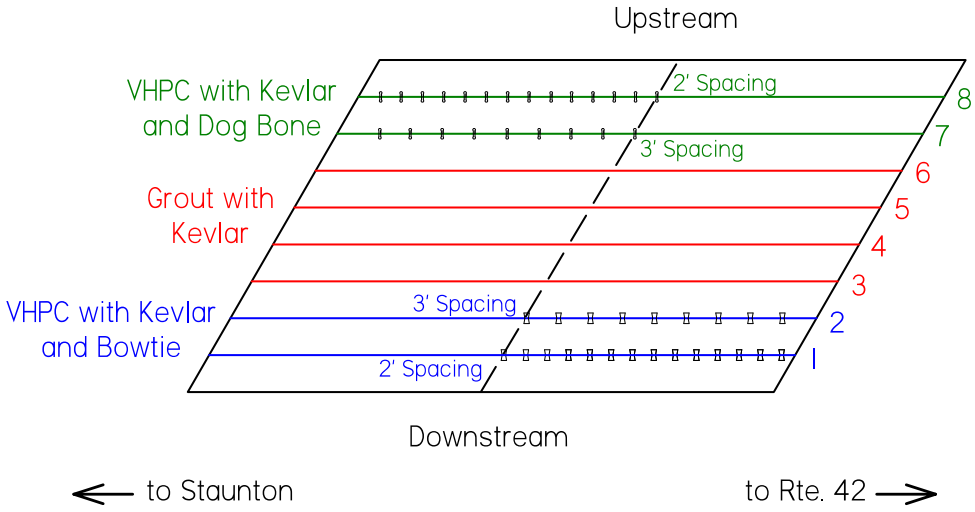

Figure 41. Buffalo Branch Bridge Rehabilitation Plan

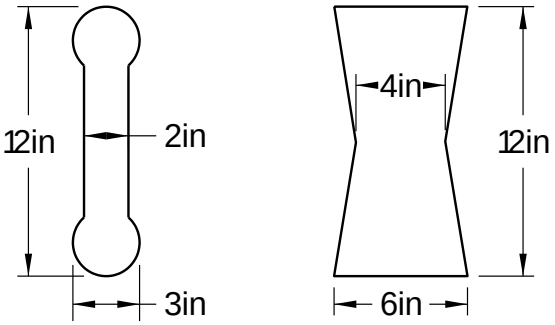

Figure 42. Cutout Geometries

The amount of VHPC required for each joint is presented in Table 10. Each batch was for 1.5 cubic ft of VHPC, which is the maximum batch size that could be mixed in the contractor's grout mixers. The researchers provided the mixing procedure presented in Table 11 to the contractor in order to ensure that VHPC placement would proceed smoothly. Note that the recommendation was that the contractor acquire two 9-cu ft capacity mortar mixers and two wheelbarrows, as well as that all constituents were weighed prior to batching. The mix design for each batch was provided and is shown in Table 12.

Table 10. Amount of VHPC Required for Joint Rehabilitation

Joint	Location	VHPC Required, ft^3	Batches Required
1	Downstream exterior	8.1	6
2	Downstream interior	7.1	6
7	Upstream interior	6.1	5
8	Upstream exterior	6.6	5

Table 11. VHPC Mixing Procedure for Buffalo Branch Bridge Rehabilitation

Start Time min	Mixer 1		Mixer 2	
	Task	Time min	Task	Time min
0	**Mixer 1 – Batch 1** Wet mixer and pour out excess water Add sand, 1⁄8-in aggregate, and half of the water and mix	5		
5	Add cement, fly ash, silica fume, and remaining water, and mix	5		
10	Add HRWR and mix Look at consistency and decide if more HRWR is desired	3	**Mixer 2 – Batch 1** Wet mixer and pour out excess water Add sand, 1⁄8-in aggregate, and half of the water and mix	5
13	Add fibers and mix	2		
15	Remove VHPC from mixer to place	5	Add cement, fly ash, silica fume, and remaining water and mix	5
18			Add HRWR and mix Look at consistency and decide if more HRWR is desired	3
20	**Mixer 1 – Batch 2** Wet mixer and pour out excess water Add sand, 1⁄8-in aggregate, and half of the water and mix	5	Add fibers and mix	2
25	Add cement, fly ash, silica fume, and remaining water, and mix	5	Remove VHPC from mixer to place	5
30	Add HRWR and mix Look at consistency and decide if more HRWR is desired	3	**Mixer 2 – Batch 2** Wet mixer and pour out excess water Add sand, 1⁄8-in aggregate, and half of the water and mix	5
33	Add fibers and mix	2		
35	Remove VHPC from mixer to place	5	Add cement, fly ash, silica fume, and remaining water and mix	5
40	**Mixer 1 – Batch 3** Wet mixer and pour out excess water Add sand, 1⁄8-in aggregate, and half of the water and mix	5	Add HRWR and mix Look at consistency and decide if more HRWR is desired	3
43			Add fibers and mix	2
45	Add cement, fly ash, silica fume, and remaining water and mix	5	Remove VHPC from mixer to place	5
50	Add HRWR and mix Look at consistency and decide if more HRWR is desired	3	**Mixer 2 – Batch 3** Wet mixer and pour out excess water Add sand, 1⁄8-in aggregate, and half of the water and mix	5
53	Add fibers and mix	2		
55	Remove VHPC from mixer to place	5	Add cement, fly ash, silica fume, and remaining water and mix	5
60			Add HRWR and mix Look at consistency and decide if more HRWR is desired	3
63			Add fibers and mix	2
65			Remove VHPC from mixer to place	5

Table 12. Mix Design for a 1.5 ft^3 Batch of VHPC-Small

Material	Details	Company	Amount, lb
Fly Ash	Class F	Titan America	13.3
Silica Fume	EMS-965	Silica Fume Association	13.3
½-in Fibers	Dramix OL 13/.20	Bekaert	14.5
Cement	Type I/II		62.3
Sand	Wytheville Sand (Passing the No. 8 Sieve)		74.7
⅛-in Aggregate	Epoxy Overlay (EP5 - Modified Sand)	Lanford Brothers	36.7
Water			17.7
High Range Water Reducer	Sika - Visco Crete 2100		650 mL
Retarder	Sika - Plastiment Water Reducing Retarder	VT	as needed

Material Properties

To measure the compressive strength, 2-in cubes were made for each batch mixed except for the final batch mixed on day two. In addition, six 3 in x 6 in cylinders were made from the final batch mixed on day two in order to measure the splitting tensile strength.

RESULTS AND DISCUSSION

This section presents the results obtained from testing and is divided into four sections: the results from the material tests, results from the non-contact splices in the sub-assemblage test, the Buffalo Branch Bridge pre-repair and post-repair live load test results, and documentation of the repair implementation.

Material Property Testing

The results from the material tests described in the Methods section are presented here. Part of the objective of the material tests was the material characterization of the VHPC mixes; therefore the two VHPC mixes are plotted separately with more detail in each section. These plots include error bars that show the values associated with the 95% confidence intervals, which were obtained using a one-sample t-test.

Compressive Strength

The results from all of the compressive strength tests performed with VHPC-Large and VHPC-Small are shown in Figure 43. Both mixes gained strength quickly and then plateaued by 14 days at about 16,000 psi. The higher variability for the VHPC-Large results is most likely due to only testing a few cylinders from a single batch between 7 and 14 days. This same batch also resulted in the lowest compressive strengths at other ages compared to the other VHPC-Large batches. Therefore, the strengths at 8 days and 12 days are not the best representation of the VHPC-Large mix overall.

The compressive strength results from all of the mixes are shown in Figure 44. The grout mixture gained strength the slowest. At 7 days, the grout had only gained about 50% of its 28-day strength while all of the other mixes had gained about 80% of their 28-day strength. It is not

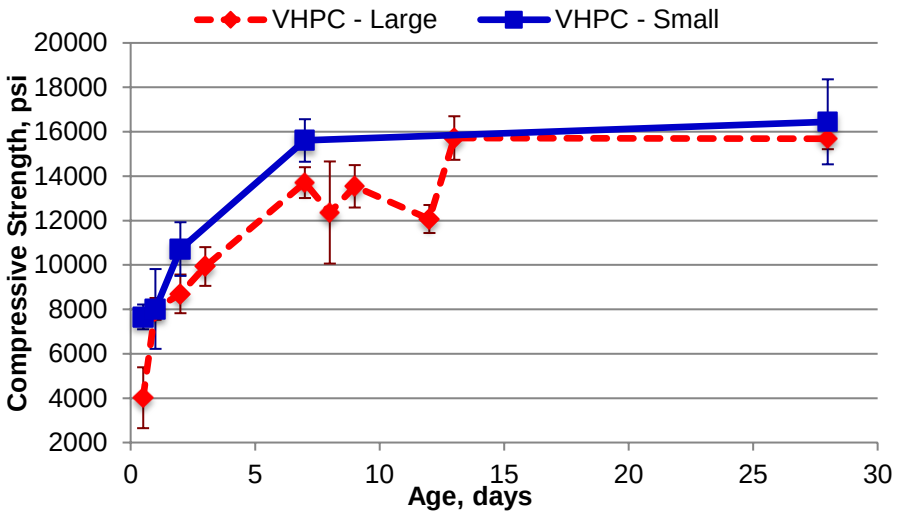

Figure 43. VHPC Compressive Strength Results

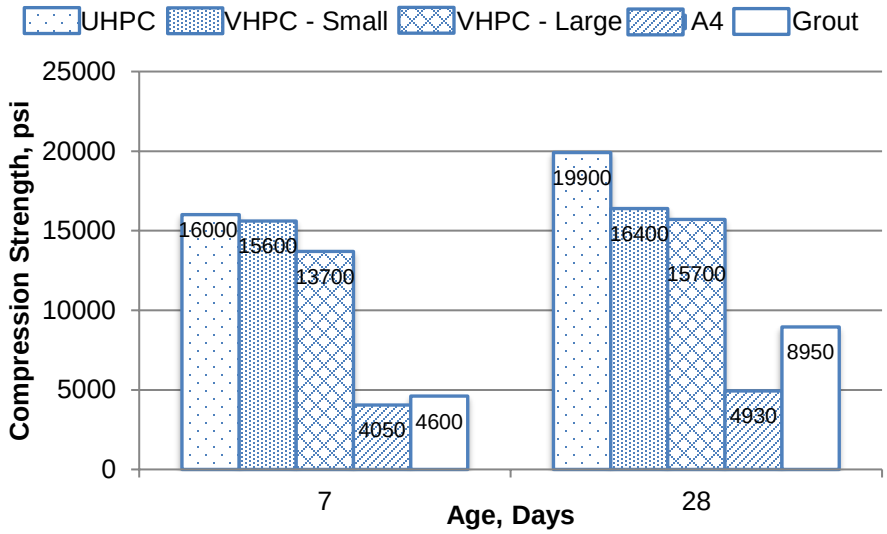

Figure 44. Compressive Strengths

known why the 28-day compressive strength of the UHPC did not meet the 21.7 ksi minimum to be considered UHPC per Graybeal (2014).

In order to gain a better understanding of how VHPC would remain workable, cure, and gain strength in different ambient temperatures, three VHPC-Small batches were mixed and left to cure outside in varying temperatures. These various temperatures mimicked the anticipated temperature environment for the Buffalo Branch Bridge rehabilitation. The high and low temperatures on the day of mixing, one day after, and two days after are presented in Table 13.

Table 13. VHPC-Small Temperatures

Mixing Date	Day of Mixing		1 Day		2 Day	
	Low, °F	High, °F	Low, °F	High, °F	Low, °F	High, °F
6/16/14	61	87	62	88	63	85
7/1/14	65	88	66	89	65	84
9/23/14	42	60	46	67	56	75

The results from the compressive strength tests are shown in Figure 45, including the mean of all the VHPC-Small batches. In comparing Table 13 with Figure 45, the VHPC-Small mixture gained strength faster with warmer temperatures and slower in colder temperatures, which could be expected. The concern was that the bridge would likely not be closed for more than just a few hours, so the VHPC would need to gain strength rapidly. Tests had not been done to determine exactly what strength was adequate for the joints, but at least 4000 psi was desired. Given this information, the researchers determined that VHPC should not be placed with temperatures below 50 °F for this type of repair project. As it happened, the repair project was delayed until the middle of the summer, so curing time was not a concern. On the other hand, VHPC does set up more quickly in warmer weather, thus decreasing the working time. The results from investigating the addition of retarder to address this issue is explained later.

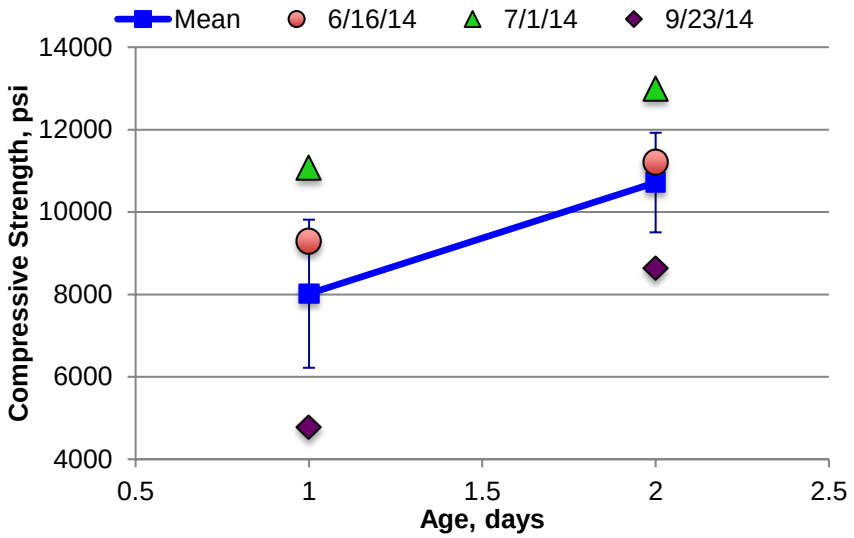

Figure 45. VHPC-Small Compressive Temperature Comparison

Splitting Tensile Strength

The splitting tensile results for both VHPC mixes are shown in Figure 46. Both VHPC mixes plateaued around 2,000 psi. The splitting tensile results at 7 days and 28 days for all of the mixes are presented in Figure 47. All of the fiber-reinforced concrete, that is UHPC and VHPC mixes, had significantly higher splitting tensile strengths than the grout and normal concrete. This result was expected because the fibers engage and can hold additional tensile force once cracking initiates. The strong tensile strength and post-cracking behavior is one of the advantages to using fiber-reinforced concretes in adjacent precast member connections instead of grout. Figure 48 presents split cylinders after testing. While the VHPC-Large cylinder is still relatively intact, the specimens with the grout and A4 concrete completely split apart at failure.

The modulus of elasticity results for both VHPC mixes are shown in Figure 49. The same cylinders tested for compressive strength were first used in the modulus of elasticity test. As discussed in the compressive strength results, cylinders tested at 12 days were tested from a single batch, which also had the lowest compressive strengths at other ages compared to the other VHPC-Large batches. As the modulus of elasticity is related to compressive strength, the lower modulus at 12 days is also explained by the weakest batch being the only one tested.

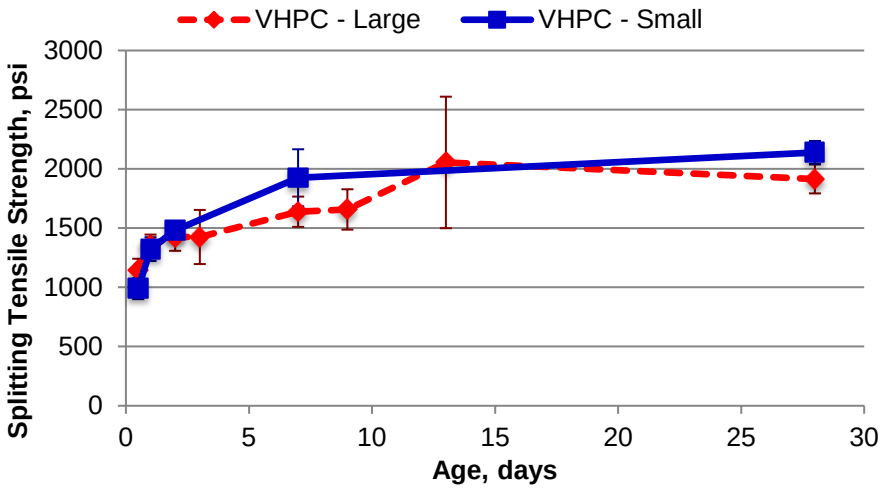

Figure 46. VHPC Splitting Tensile Results

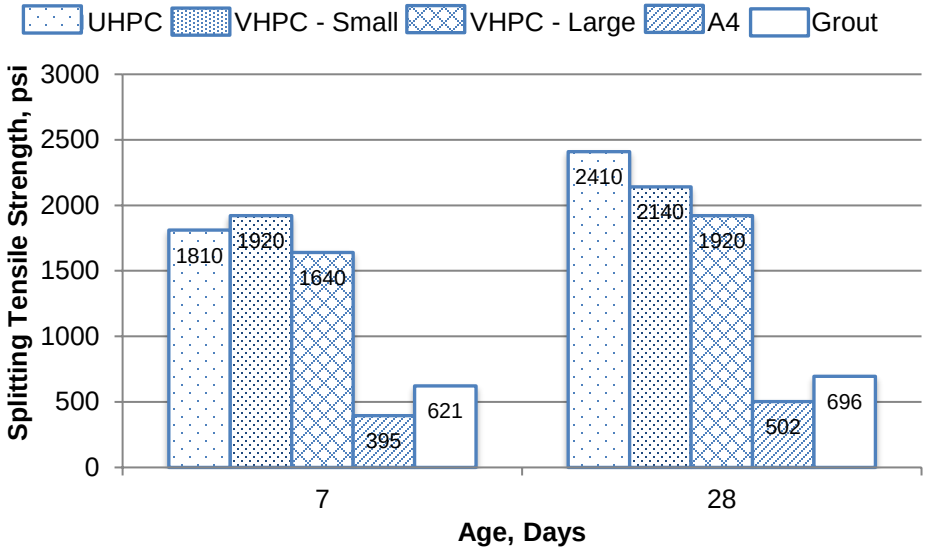

Figure 47. Splitting Tensile Strengths for All Mix Designs

(a) **(b)** **(c)**

Figure 48. (a) Grout, (b) A4, and (c) VHPC-Large Sample Cylinders, After Tensile Splitting Strength Tests

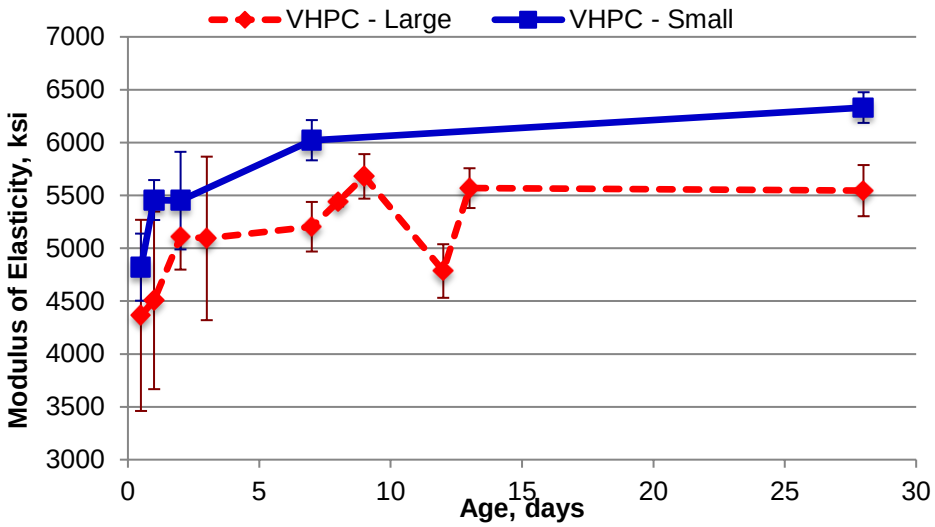

Figure 49. VHPC Modulus of Elasticity

Modulus of Elasticity

The modulus of elasticity results for all of the mixes at 7 days and 28 days are shown in Figure 50. The modulus of elasticity for UHPC exhibited a larger difference relative to the other mixes compared to the difference previously seen in the strength tests. Also note that the grout had a 28-day compressive strength that was almost double that of the A4 deck concrete, even though the modulus of elasticity for the grout was the lower of the two. This is most likely due to the added stiffness provided by the coarse aggregate in the A4 mix.

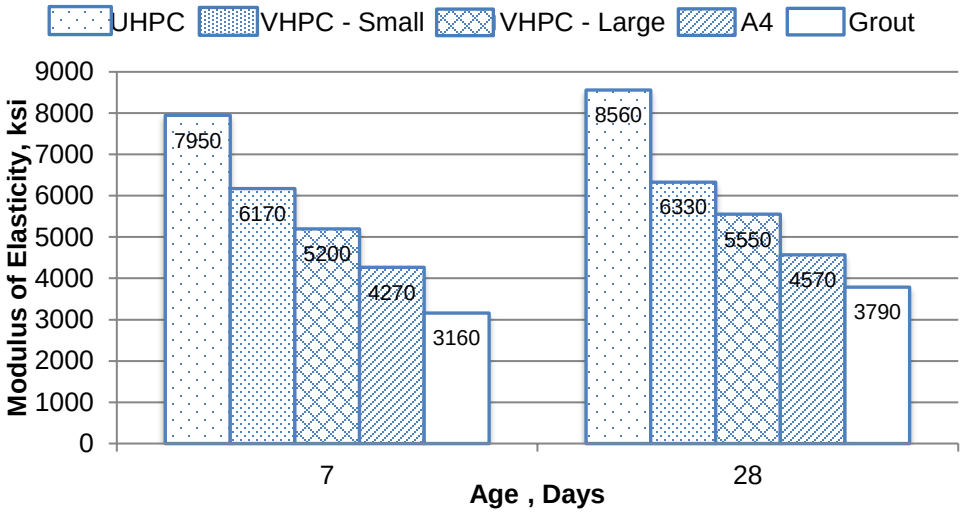

Figure 50. Modulus of Elasticity

Reinforcing Steel Bond

The pull out tests were performed on VHPC-Large and VHPC-Small specimens at ages ranging from 12 hr to 7 days. The reinforcing steel ruptured in each test. Figures 51 and 52 present the data for the VHPC-Large mixture from the wire pot and bottom LVDT, respectively. The first test at 12 hours ruptured the reinforcing steel without exhibiting slipping at the bottom

more than 0.005 in. Unfortunately, the actuator began to leak oil during the second test at 1 day. So, the specimen was unloaded and the actuator was temporarily fixed to finish testing. However, the actuator was still leaking oil at day 2, causing the test to be postponed until day 7, when the actuator was permanently fixed.

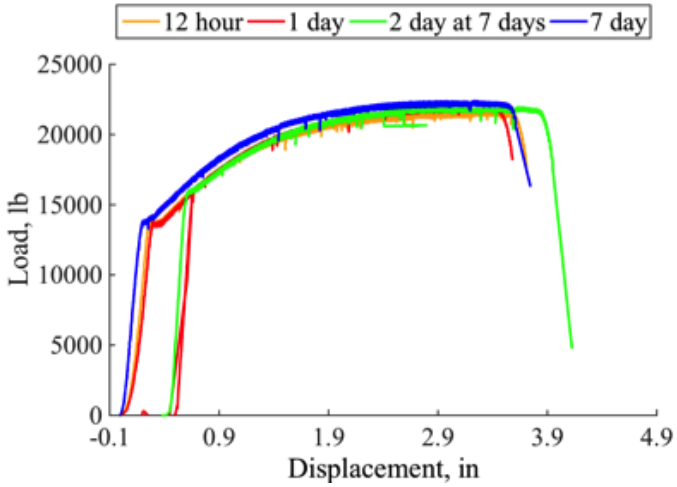

Figure 51. VHPC Large –Wire Pot versus Load

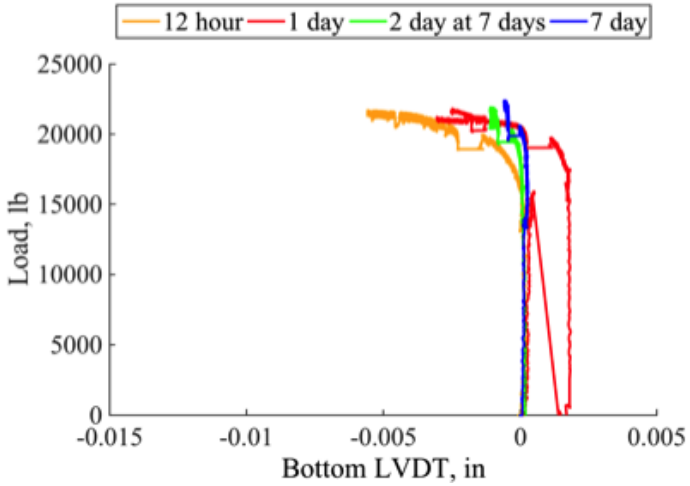

Figure 52. VHPC Large —Bottom LVDT versus Load

Figures 53 and 54 present the data for the VHPC-Small mixture from the wire pot and bottom LVDT respectively. The first test at 12 hr ruptured the reinforcing steel and only had 0.01 in slip at the bottom LVDT. The reinforcing steel used in the 1-day specimen ruptured at a load that was much lower than every other Grade 60 steel bar used in testing, which typically ruptured around the expected load of 20 kips. The No. 4 bars have a cross-sectional area of 0.2 in^2 and an expected breaking strength of around 100 ksi, so load to cause rupture should be around 20 kips. After testing, the researchers examined the steel for the 1-day specimen and found that the cause for the early failure was a deformity where the steel had ruptured. Nevertheless, the results for both VHPC mixes showed that adequate bond between the VHPC and reinforcing steel was obtained within 12 hours.

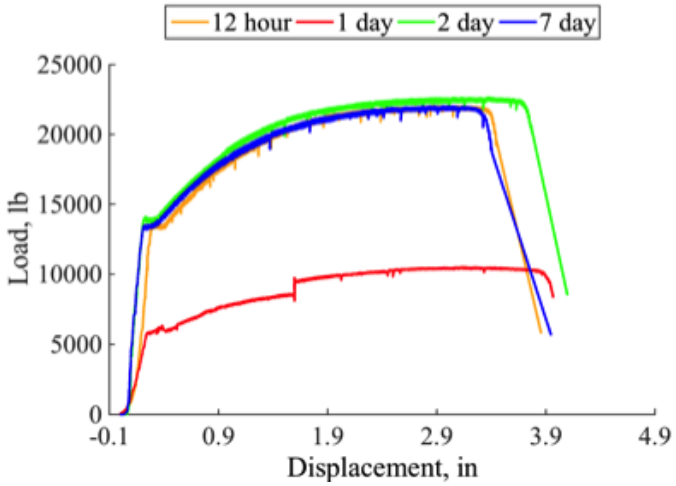

Figure 53. VHPC Small--Wire Pot versus Load

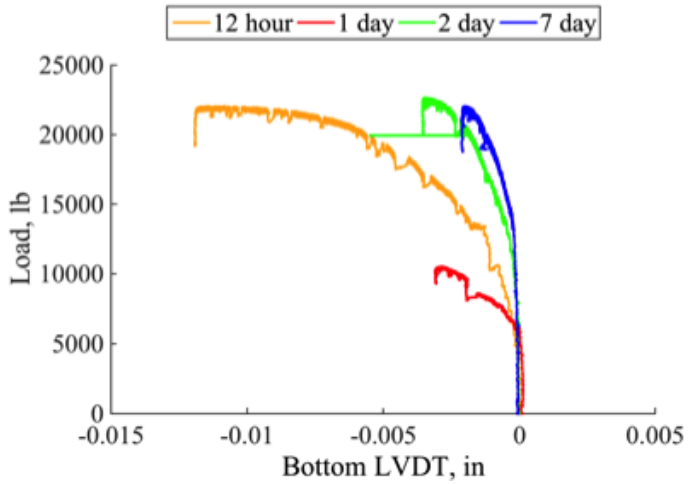

Figure 54. VHPC Small--Bottom LVDT versus Load

Bond with Concrete

The results of the pull off tests for both VHPC mixes are shown in Figure 55. The surface preparation that improved the bond strength the most was SSD. At 28 days, the combination of sand blasting and SSD only improved the bond strength by 20% compared to not sand blasted but SSD. The time and effort required to sand blast an entire shear key surface is an uneconomical option for only a 20% increase in strength. On the other hand, the time and effort required to create an SSD surface at the shear key is minimal, given the significantly greater bond strength at seven days for sand blasted or not sand blasted with SSD compared to the dry sand blasted surface.

Joyce (2014) performed the same pull off tests for UHPC, grout, and VHPC-Large with a sand blasted and SSD surface condition. The results are shown in Figure 56. With the same surface conditions, UHPC and VHPC-Large had the same bond strength, while the grout had less than 10% of the bond strength at 15 days.

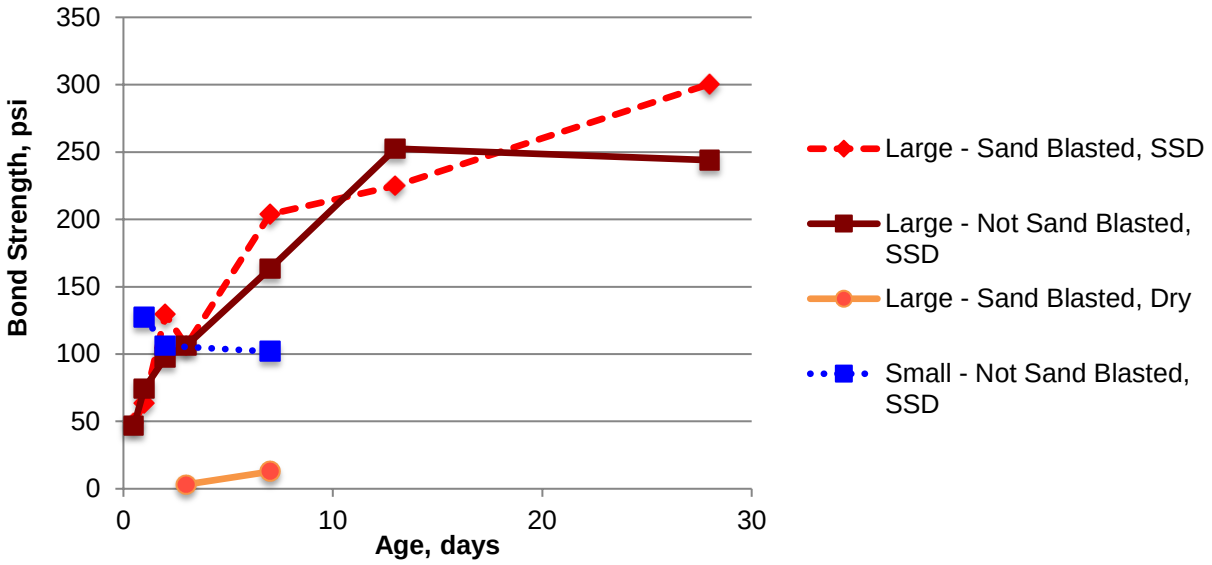

Figure 55. VHPC Bond with Concrete

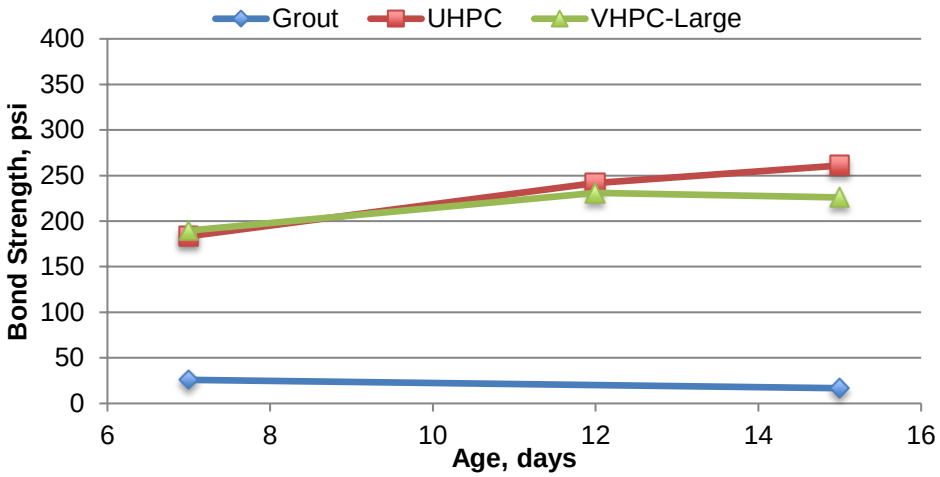

Figure 56. Joyce Bond Tests Results (2014)

According to finite element analysis performed by Halbe (2014), the expected tensile stress at the base of the key was approximately 180 ksi under HS-20 loading including dynamic load allowance. The VHPC and UHPC attained this bond strength at 7 days, but the typical grout did not.

The VHPC failure classifications experienced in these tests are presented in accordance with ASTM D7234 (2012b). The typical failure mode observed at 12 hours and one day was substrate failure C, in which the bond failed at a thin layer of cementitious material from the original concrete. This failure mode is shown in Figure 57. Unfortunately, a few of the 12-hour tests failed at the epoxy because there was not adequate time for the adhesive to fully cure.

The typical failure mode observed in the VHPC at two days to five days was substrate failure B, in which the bond failed at the cement paste but was not strong enough to fracture the aggregate, as depicted in Figure 58.

Figure 57. Typical VHPC 12-Hour to 1-Day Failure

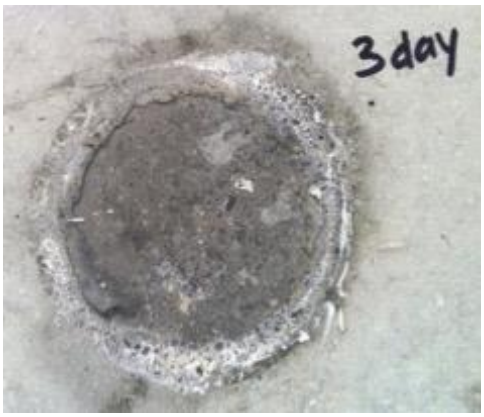

Figure 58. Typical VHPC 2-Day to 5-Day Failure

The typical failure mode observed in the VHPC at seven days and older was substrate failure A, in which the bulk of the cement paste was detached along with fracturing the aggregate inside the precast concrete member. This failure type is shown in Figure 59, where the left two pictures were taken at seven day tests and the picture on the right was taken at 28 days.

Figure 59. Typical VHPC 7-Days and Older Failure

Workability and Flow

The results for the inverted slump tests are shown in Figure 60. Time zero represents when the VHPC was fully mixed and could be placed. The first test of the VHPC-Large mixture showed that by 30 minutes the spread had decreased to 14 in and no longer flowed as desired. Thus, adding retarder to the mix was then investigated. Like HRWR, the retarder was dosed in units of oz/cwt, and the quantity added is denoted in the plot by the number next to the mix, with "0" meaning no retarder was added. After observing that the retarder did not improve the workability after the mix sat still for 20 minutes, the investigators examined continuously mixing the VHPC. Originally, the VHPC was left without agitation in the mixer for 10 minutes in between tests. However, for the "Mixed" batches noted in the plot, the mixer was left on throughout the tests. Doing so greatly improved the workability as time elapsed. The tests were also performed on a continuously mixed VHPC-Small mix without retarder. The VHPC-Small performed significantly better than the VHPC-Large and did not lose much of its workability after 40 minutes. The initial target spread for the VHPC was determined to be 19 in to 21 in.

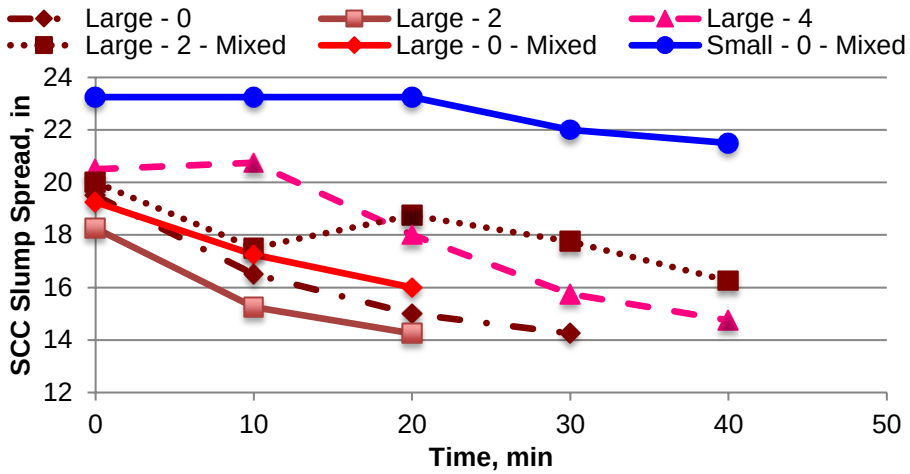

Figure 60. VHPC Slump Spread for Various Amounts of Retarder Added and Degree of Mixing

In addition to workability time, another objective was to determine how far the mixture could reasonably be expected to flow. The results of the box flow tests with the VHPC-Large mixture are shown in Figure 61. As can be seen, the addition of retarder along with continuously mixing the VHPC-Large greatly improved the workability of the mix.

The results from the shear key flow test with the VHPC-Small mixture are shown in Figure 62. Placing the VHPC-Small began in the low end and moved toward the upper end. The majority of the shear key was continuously placed; however, the upper end was placed after a fifteen minute break. The transverse slope of the geometric cutouts was also found to not cause the VHPC to overflow on the low end. A picture of this is shown in Figure 62 where the VHPC-Small is still level after being placed on an incline.

To examine what happened when two batches were placed next to each other, the top half of the joint was rodded while the bottom half was not. The results of this are shown in Figure 63. As can be seen, a cold joint formed on the bottom half of the upper end where the two batches were not rodded together.

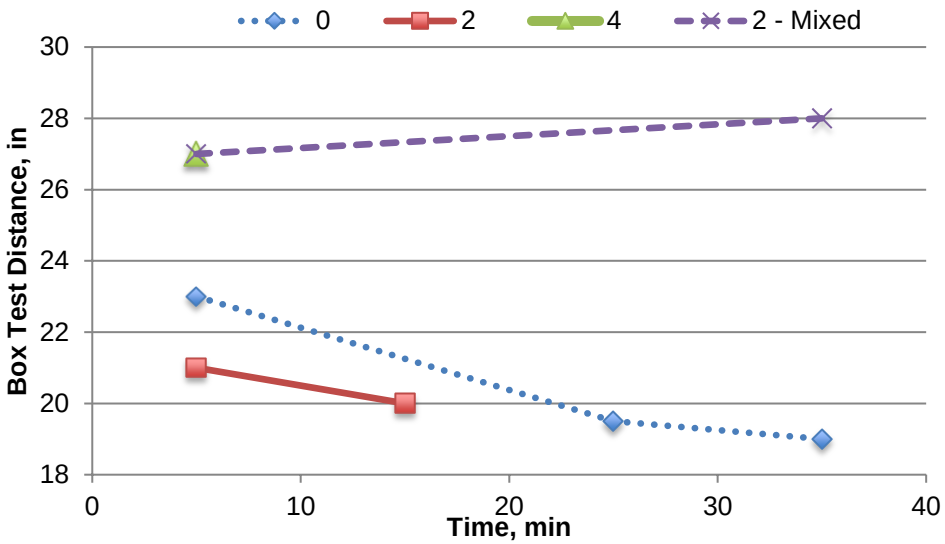

Figure 61. VHPC-Large Box Flow Tests Results (Number in Legend Indicates oz/cwt of Retarder)

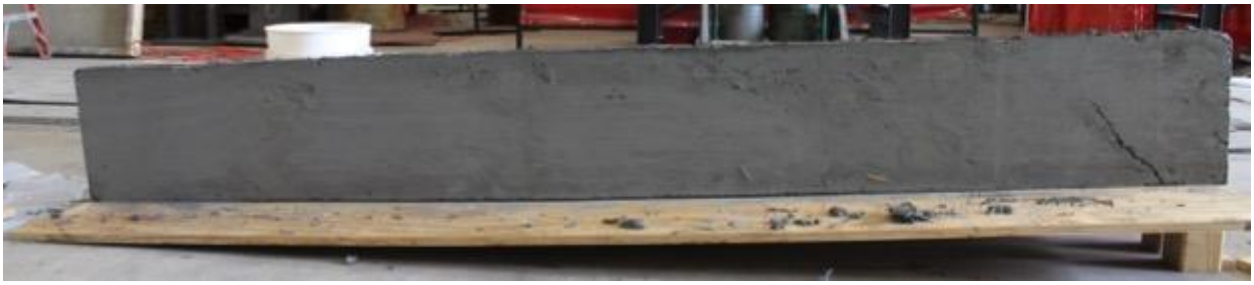

Figure 62. Shear Key Flow Test Overall After Removing the Formwork

Figure 63. Shear Key Flow Test Lower End (Left) and Upper End (Right)

Shrinkage

The shrinkage tests results are shown in Figures 64 through 66. As mentioned before, not all of the specimens that were cast for this test were able to be measured in the ASTM C157 specified testing comparator, due to exceeding the tolerances for length. Nevertheless, the shrinkage results for those samples that were tested in comparator are shown in 64. The UHPC and VHPC mixes showed the highest shrinkage, which was due to their higher concentration of cementitious materials.

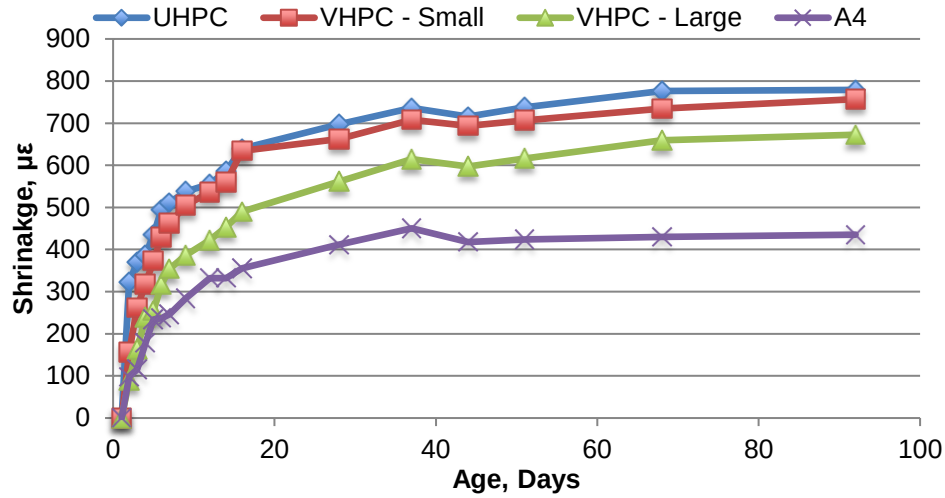

Figure 64. Average Shrinkage Measured Using Comparator Apparatus

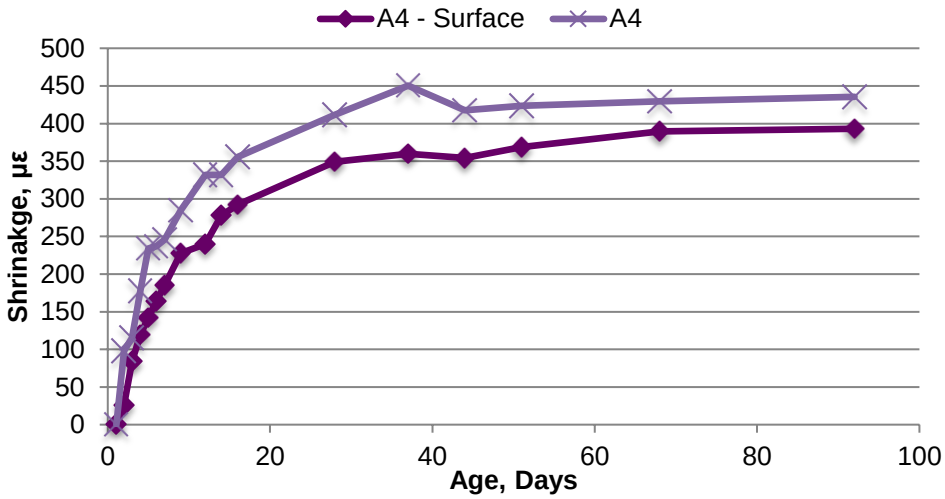

Figure 65. Shrinkage Methods Comparison

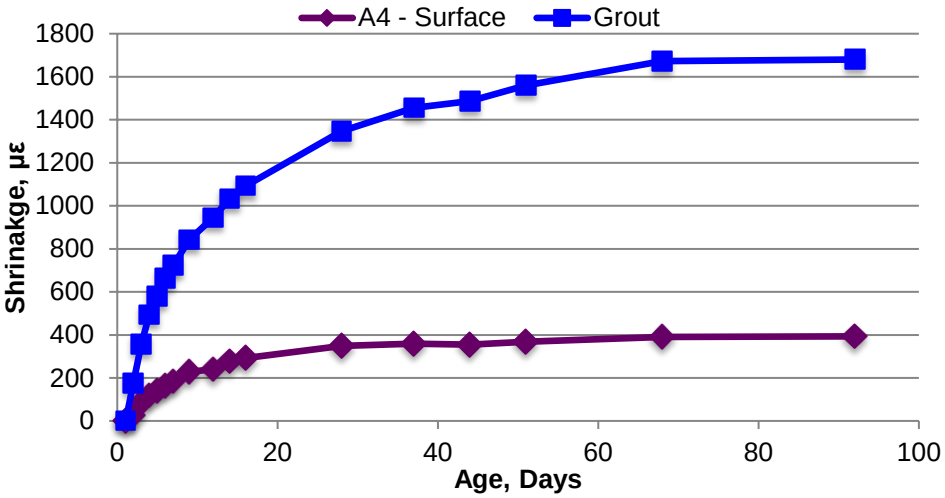

Figure 66. Surface Shrinkage

As a comparison in methods, one of the A4 specimens included in Figure 64 was also fitted with DEMEC discs epoxied to the specimen surface. The researchers then determined the shrinkage along the surface of that specimen and analyzed those results with the measurements using the comparator. Figure 65 shows that the difference of the two test methods for measuring shrinkage was very small and could be considered negligible. Therefore, the grout specimens that were also measured for shrinkage using DEMEC discs, and whose results are presented in Figure 66, can be directly compared to the shrinkage results of the VHPC in Figure 64.

Interestingly, the grout was marketed as a non-shrink precision grout; however, the material exhibited more than four times as much shrinkage as the A4 deck concrete and over twice as much as the UHPC and VHPC mixes. This comparison is one indicator that shrinkage cracks are more likely to form in the grout, which is therefore not the best material to use in the shear keys.

Durability

The results from the freeze/thaw tests are shown in Figure 67 through Figure 69. Based on the work conducted by Lane and Ozyildirim (1999) and ASTM C666 (2008), the durability factor after 300 cycles should be greater than 60. The durability factor is defined as the ratio of the dynamic modulus divided by the original dynamic modulus, expressed as a percentage. As seen in Figure 67, all of the tested mixes had durability factors above 90 after 300 cycles.

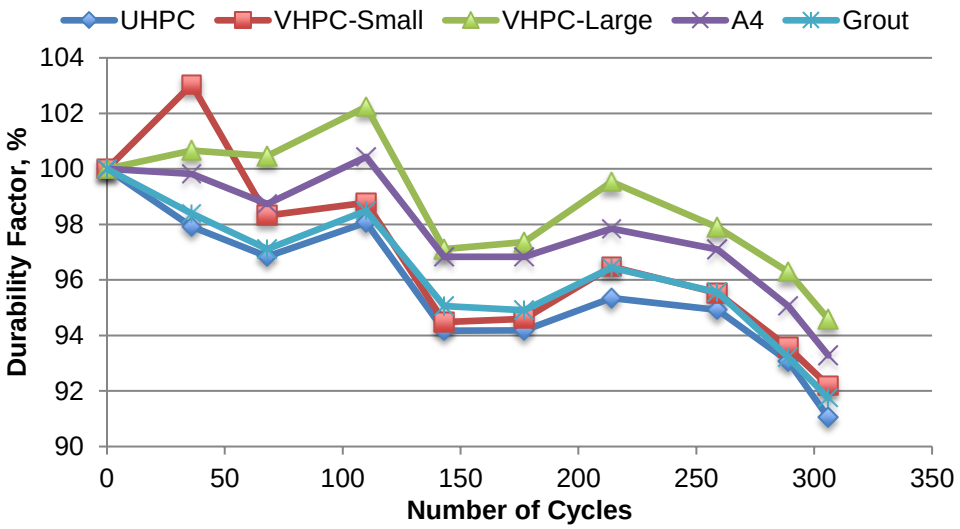

Figure 67. Freeze/Thaw Relative Dynamic Modulus

In addition to assessing freezing and thawing resistance through dynamic moduli, the researchers also examined scaling by weighing specimens that were initially dry, and then after each group of freezing and thawing cycles. After removing the specimens from the water, the surface was dried, and the scaled surface was wiped. As seen in Figure 68, the weight measurements taken after the first group of cycles show that some of the specimens absorbed a large amount of water. The weights then remained constant until the surfaces of the specimen started scaling.

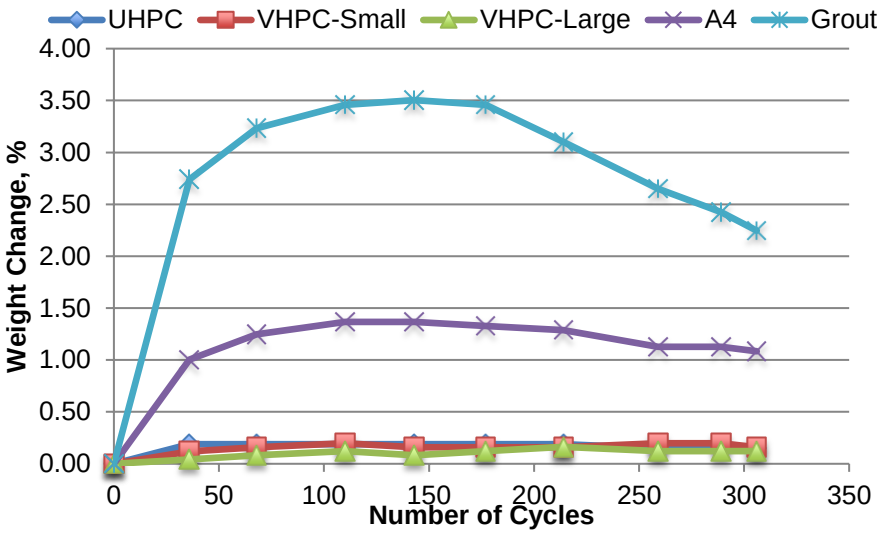

Figure 68. Freeze/Thaw Weight Change

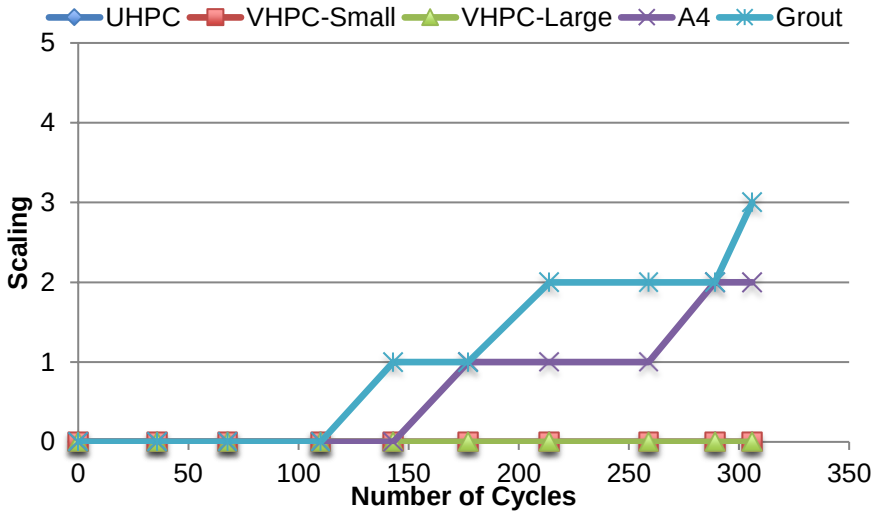

Figure 69. Freeze/Thaw Scaling

The data presented in Figure 69 indicates the degree of scaling of the bottom and side surfaces of the specimens; none of the top surfaces exhibited scaling because they were not fully submerged for the entirety of testing. The ASTM C672 (2012a) rating system for scaling was as follows:

- 0 = no scaling
- 1 = very slight scaling, no coarse aggregate visible
- 2 = slight to moderate scaling
- 3 = moderate scaling, some coarse aggregate visible
- 4 = moderate to severe scaling
- 5= severe scaling, coarse aggregate visible over entire surface.

The grout and UHPC did not have aggregate to be exposed, so the rating system was adjusted to a judgment call of whether or not the amount of scaling would have caused the

aggregate to be exposed. While the UHPC and both VHPC mixes did not exhibit any scaling in the first 300 cycles, the steel fibers that were exposed began to rust.

Cost Assessment of VHPC

While the material properties for VHPC and UHPC tend to be similar, the main advantage of VHPC as opposed to UHPC is the cost. As previously mentioned, VHPC is a non-proprietary mixture that can be easily mixed using readily available materials and also has the addition of coarse aggregate. The cost of the materials required to make 1 yd^3 of VHPC is presented in Table 14 and Table 15. Note that the majority of the cost comes from the steel fibers. A 50-lb bag of non-shrink grout costs approximately $14 and yields 0.45 ft^3 (Home Depot, 2017). Based on this, one cubic yard of this type of prebagged grout would cost $840. This is based on retail cost, and it might be possible to obtain the grout at lower cost buying in bulk.

Table 14. VHPC - Large Cost

Material	Amount, lb/yd^3	Cost, $/lb	Total Cost, $/$yd^3$
Water	319	0	0.00
Cement	1121	0.0625	70.03
Fly Ash	240	0.0300	7.21
Silica Fume	240	0.2100	50.46
Sand	1450	0.0098	14.14
¼ in Limestone	621	0.0093	5.74
1.2 in Fibers	265	1.1173	295.64
HRWR (25 oz/cwt)	11836	0.0040	46.47
		Total Cost:	**490**

Table 15. VHPC - Small Cost

Material	Amount, lb/yd^3	Cost, $/lb	Total Cost, $/$yd^3$
Water	319	0	0.00
Cement	1121	0.0625	70.06
Fly Ash	240	0.0300	7.20
Silica Fume	240	0.2100	50.40
Sand	1345	0.0098	13.11
⅛ in Limestone	660	0.0610	40.26
½ in Fibers	260	2.3100	600.60
HRWR (25 oz/cwt)	11727	0.0040	46.47
		Total Cost:	**828**

Material Tests Summary

A summary of the material test results is presented in Table 16. As observed previously, the UHPC and both VHPC mixes gained strength faster and achieved higher compressive and

splitting tensile strengths than the grout. The splitting tensile tests for the UHPC and both VHPC mixes also exhibited some post cracking tensile strength where the steel fibers bridged the cracks so that the cylinders continued to take load. Along with the greater strengths, the UHPC and both VHPC mixes also had higher moduli of elasticity than the grout. While the superior compressive and splitting tensile strengths make the high performance concrete mixes a better option than grout, the bond strength with the concrete is their greatest advantage. Because the deterioration of the grout shear key begins at the bond with the precast concrete member, the stronger bond strength could potentially make the joints last significantly longer. The bond strength of the UHPC and both VHPC mixes to existing concrete tends to be about 10 times larger than the bond of the grout. The durability as measured with the relative dynamic modulus shows that after 300 cycles all of the mixes were still intact. However, of the four mixes, the grout was the only one that presented scaling. The shrinkage exhibited by the non-shrink grout far exceeded that of the UHPC and both VHPC mixes. Given the small differences with UHPC in terms of material properties, VHPC was the more economical option compared to its proprietary cousin.

Table 16. Material Properties Summary

Average Material Properties	Age, days	UHPC	VHPC-Small	VHPC-Large	Grout
Compressive Strength, psi	7	16000	15600	13700	4600
	28	19900	16400	15700	8950
Splitting Tensile Strength, psi	7	1810	1920	1640	621
	28	2410	2140	1920	696
Modulus of Elasticity, ksi	7	7950	6170	5200	3160
	28	8560	6330	5500	3790
Bond with Concrete, psi (sand blasted, SSD)	7	183	102[1]	190	26
	15	261	N/A	226	17
Relative Dynamic Modulus, %	300 cycles	91	92	95	92
Shrinkage, με	7	511	462	354	724
	28	698	662	561	1347
	92	779	757	673	1680
Cost, $/yd^3	N/A	2000[2]	828	490	840

[1]VHPC-Small Bond results were for non-sandblasted, SSD.
[2]Cost estimate for proprietary UHPC, includes engineering with project.

Cyclic Tests of Non-Contact Lap Splice Connection

An initial static test was performed and then the specimen was loaded with 1,000,000 cycles of load as outlined in the Methods section and a final static test was performed. The research team conducted static tests on the sub-assembly of voided slab sections before and after an intermittent series of cyclic tests up to 1,000,000 cycles. However, the objective of the lap splice testing was to compare the overall performance of the non-contact lap splice to that of the contact lap splice (Joyce, 2014). Therefore, only the results from the final static tests are presented in this report. Note that both specimens were unable to reach total failure due to the load frame capacity.

Cracks were first observed in the contact lap splice specimen on both faces of the north joint at an actuator displacement of 0.09 in, while the south joint remained uncracked until 0.25 in (Joyce, 2014). Cracks first formed at the interface of the precast concrete and the VHPC in the bottom of the shear keys. As the tests continued, the cracks propagated into the precast concrete member instead of the stronger VHPC shear key. Splitting cracks were also observed in the VHPC on top of the south blockout above the lap splice bar. The largest joint opening measured before the test was terminated was 0.123 in across the north joint.

Similarly to the contact lap splice test, the non-contact lap splice test specimen began to crack at an actuator displacement of 0.08 in, although cracking first initiated in the south joint while the north joint remained uncracked until 0.27 in of actuator displacement. Again, the cracks initiated at the interface of the precast concrete and the VHPC in the bottom of the shear keys and propagated into the precast concrete member as the test continued. The non-contact lap splice test had the same maximum joint opening of 0.123 in. Figure 70 and Figure 71 show the displacements of the joint LVDTs during the final static tests of both specimens. Although both test specimens exhibited cracking during testing, the water ponding tests showed no signs of water leaking through the joints.

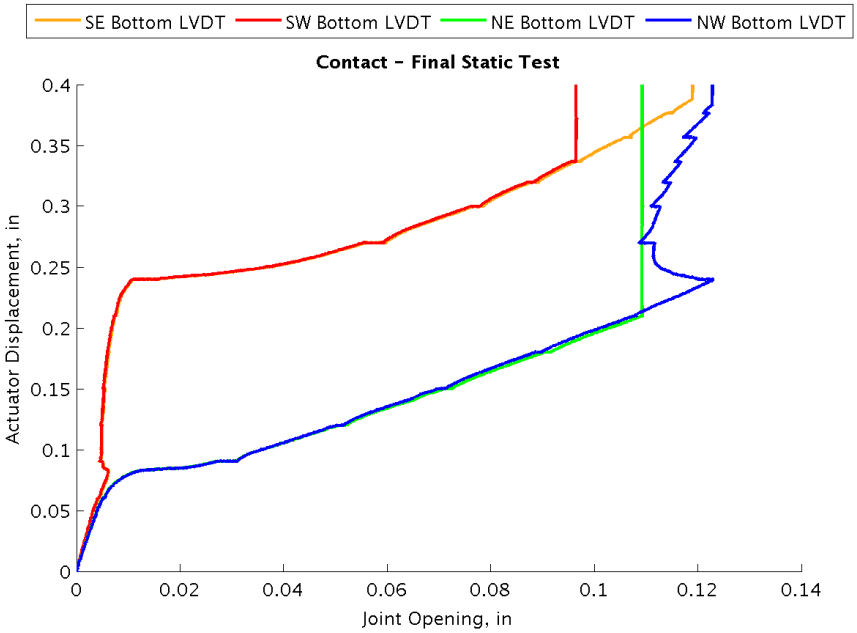

Figure 70. Contact Splice Final Static Test (Joyce, 2014)

A comparison of the actuator load and displacement of the contact and non-contact lap splice tests is shown in Figure 72. The maximum load reached for the contact lap splice test was 32,400 lb at 0.44 in of actuator displacement. For the non-contact lap splice test, the results were 25,600 lb at 0.36 in. According to Joyce, the service load was calculated to be 3800 lb, which both specimens clearly exceeded. Again, neither specimen was loaded to failure due to the capacity of the test set up, but the non-contact lap splice testing ended at a smaller load. The displacement of the non-contact lap splice specimen was only slightly higher than that of the contact lap splice specimen under the same load and both followed the same linear slope. These results provide a good indication that a shear key with a non-contact lap splice will perform as well as one with a contact lap splice.

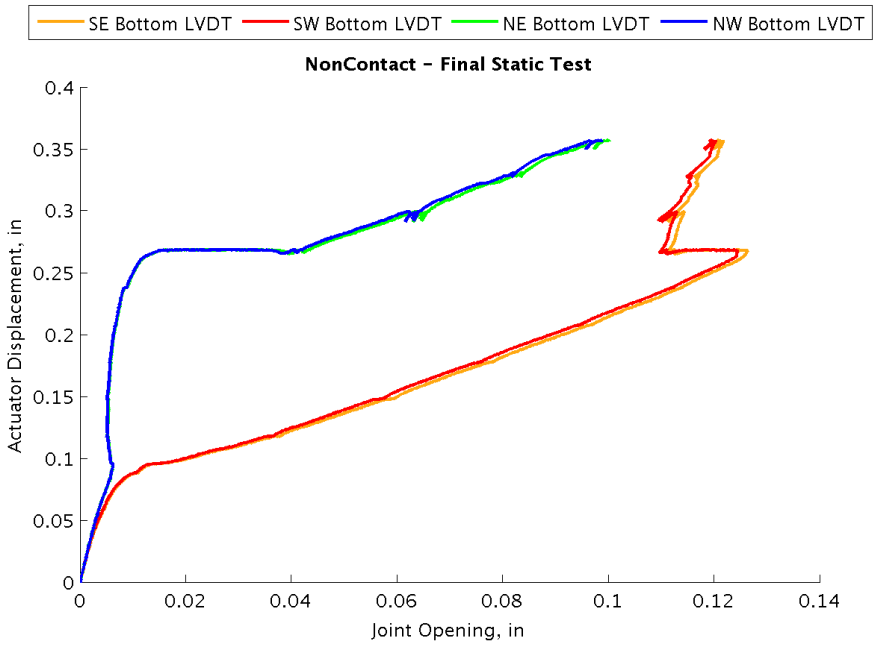

Figure 71. Non-Contact Splice Final Static Test

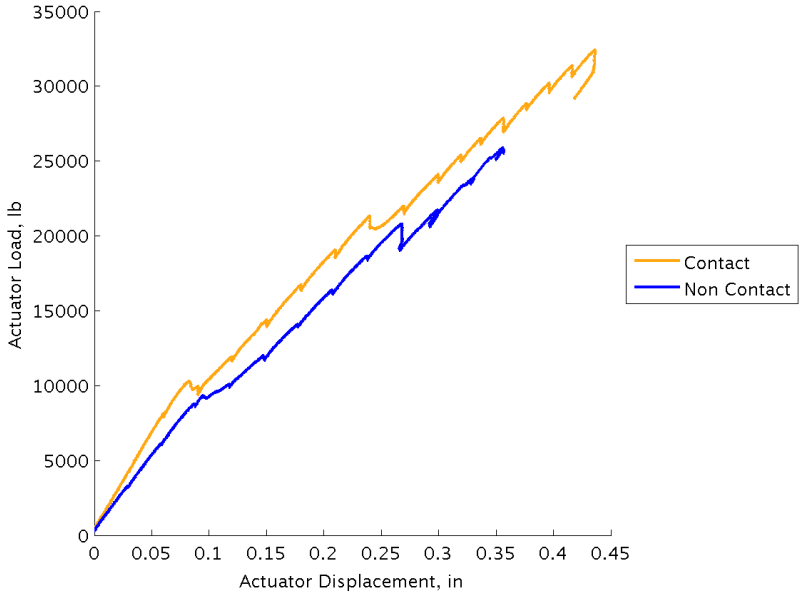

Figure 72. Contact versus Non-Contact Final Static Test

Buffalo Branch Bridge Live Load Tests

Live load tests of the Buffalo Branch Bridge were conducted before and after the repair of the longitudinal joints. This section presents the measured strains, displacements and relative joint displacements from the live load tests.

Strains and Displacements

Figures 73 through 84 present comparisons of the pre-repair (initial) and post-repair responses of the bridge. For each test, there were some sensors that gave unreliable readings and thus, are not presented. The plotted lines are the averages of the three truck crossings for each load case. As can be seen in the plots, the pre- and post-repair behaviors were fairly similar, except for the behavior of Beam 1. Recall that the worst joint was between Beam 1 and Beam 2, and Load Cases 1 through 3 were the three cases that most directly loaded that side of the bridge. Under those loading situations, the deflections and strains in Beam 1 were smaller in the pre-repair condition than the post-repair condition. Because the load trucks were adjacent to or nearby, but never directly on, Beam 1, these results indicate that post-repair, the beam was better tied to the system and carried a larger percentage of the total load. For Load Cases 4 through 6, there was not a significant difference in behavior because the joints on that side of the bridge were in much better pre-repair condition.

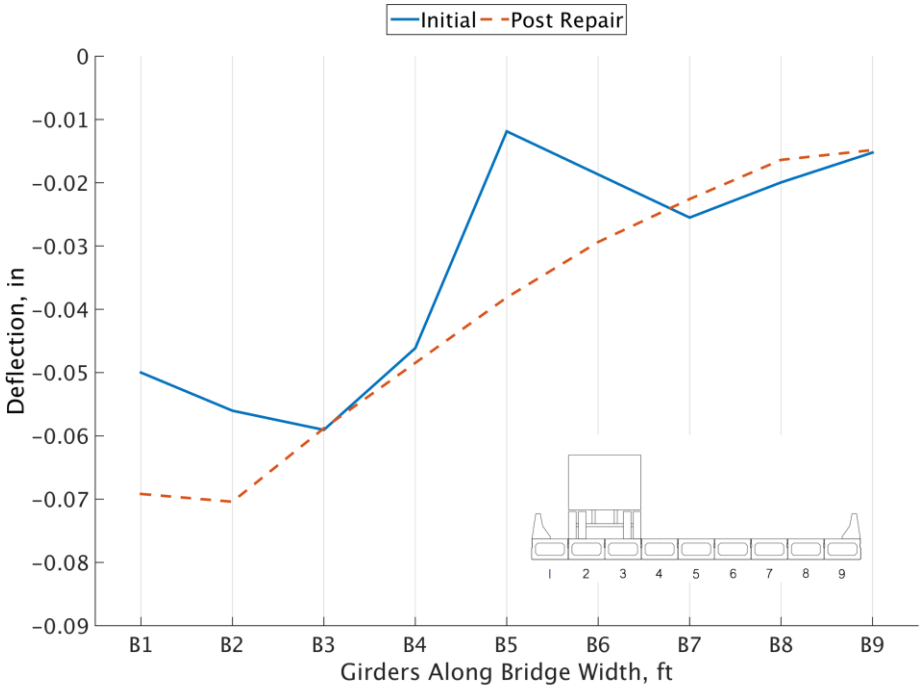

Figure 73. Load Case 1 Deflection Comparison

Linear Variable Differential Transformers

The horizontal and vertical relative displacements of adjacent box beam members at the two exterior longitudinal joints on both sides of the bridge were measured for each of the three runs of the six load cases. The results are presented in Figures 85 through 88. In the figures, the solid lines are used for Load Cases 1 through 3, where the load trucks were positioned on the downstream side of the bridge. Dashed lines are used for Load Cases 4 through 6, where the load trucks were positioned on the upstream side of the bridge. Also note in the figures that mirror image load cases have the same marker shapes, for easier comparisons.

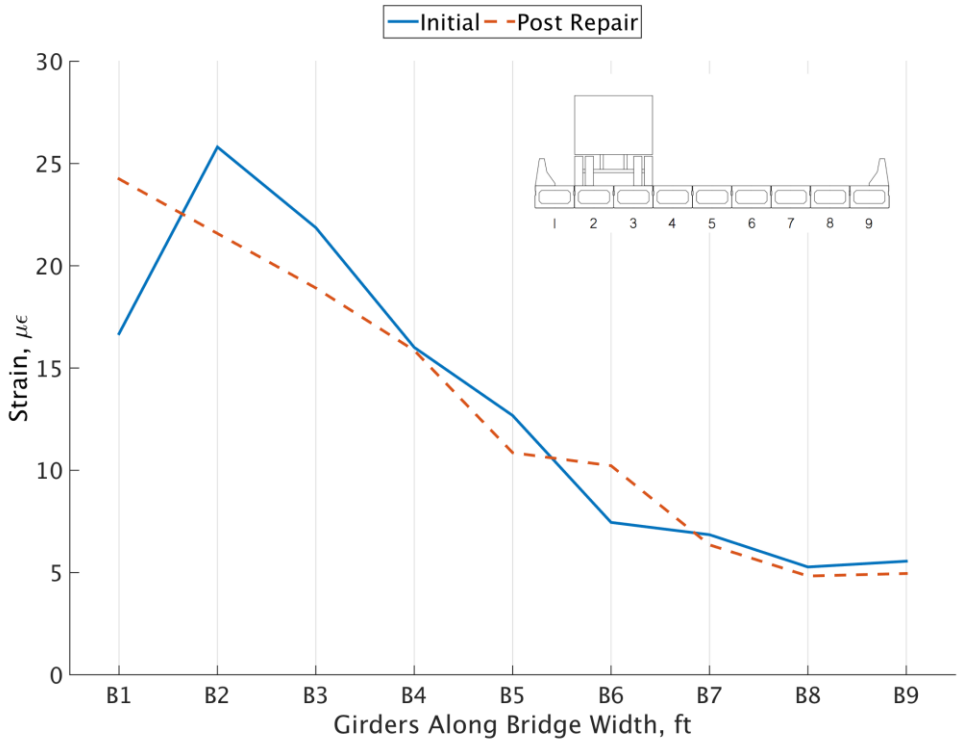

Figure 74. Load Case 1 Strain Comparison

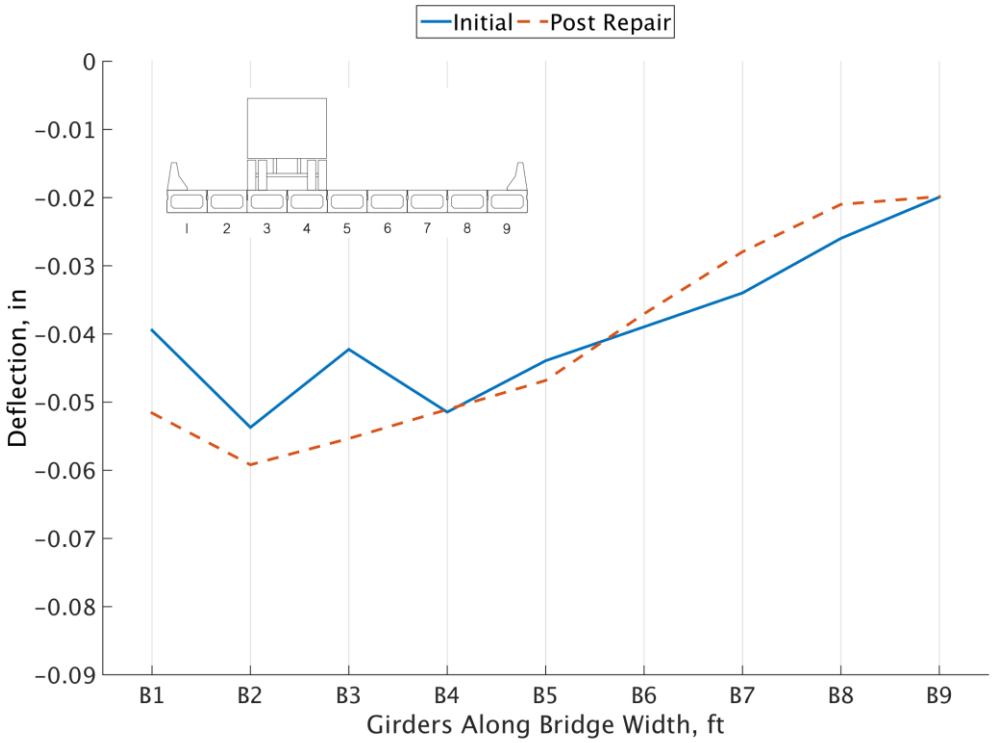

Figure 75. Load Case 2 Deflection Comparison

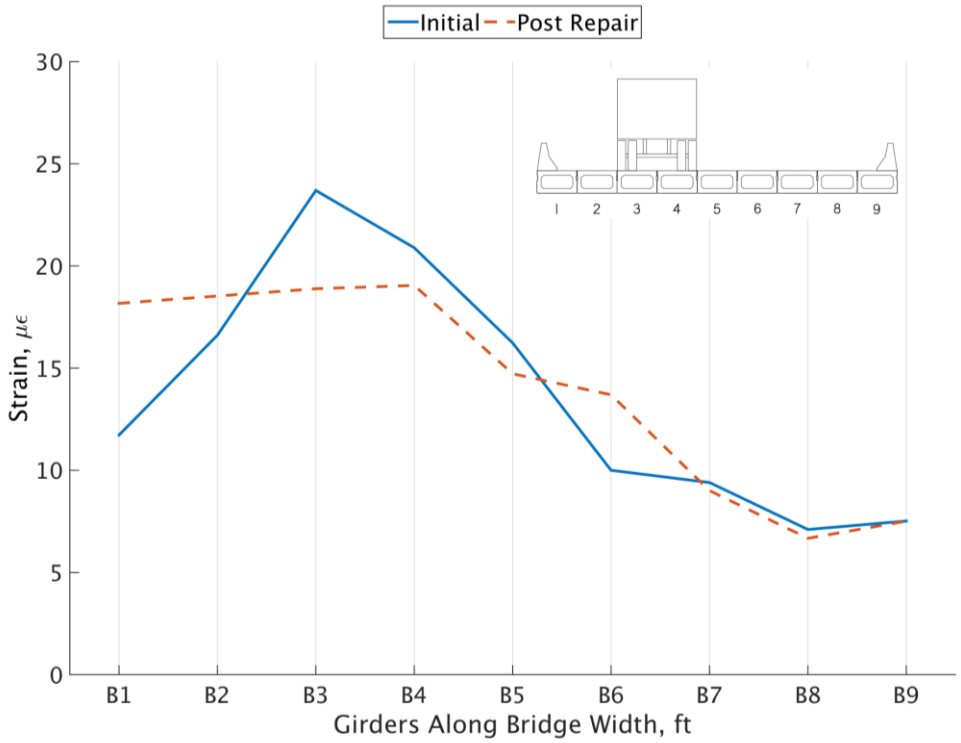

Figure 76. Load Case 2 Strain Comparison

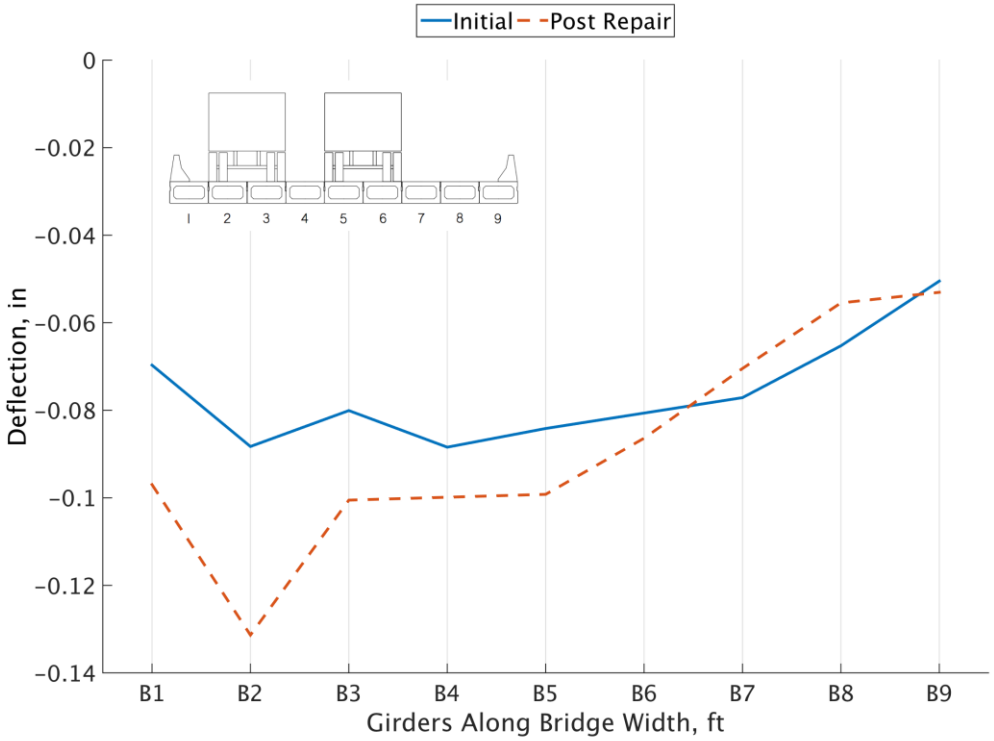

Figure 77. Load Case 3 Deflection Comparison

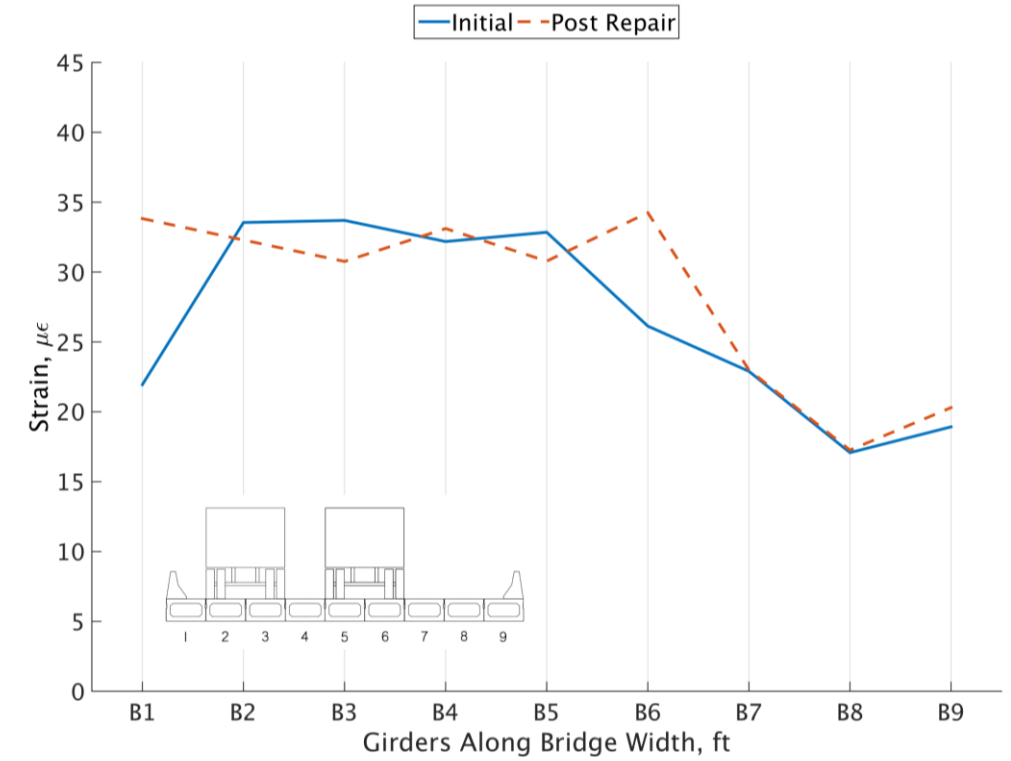

Figure 78. Load Case 3 Strain Comparison

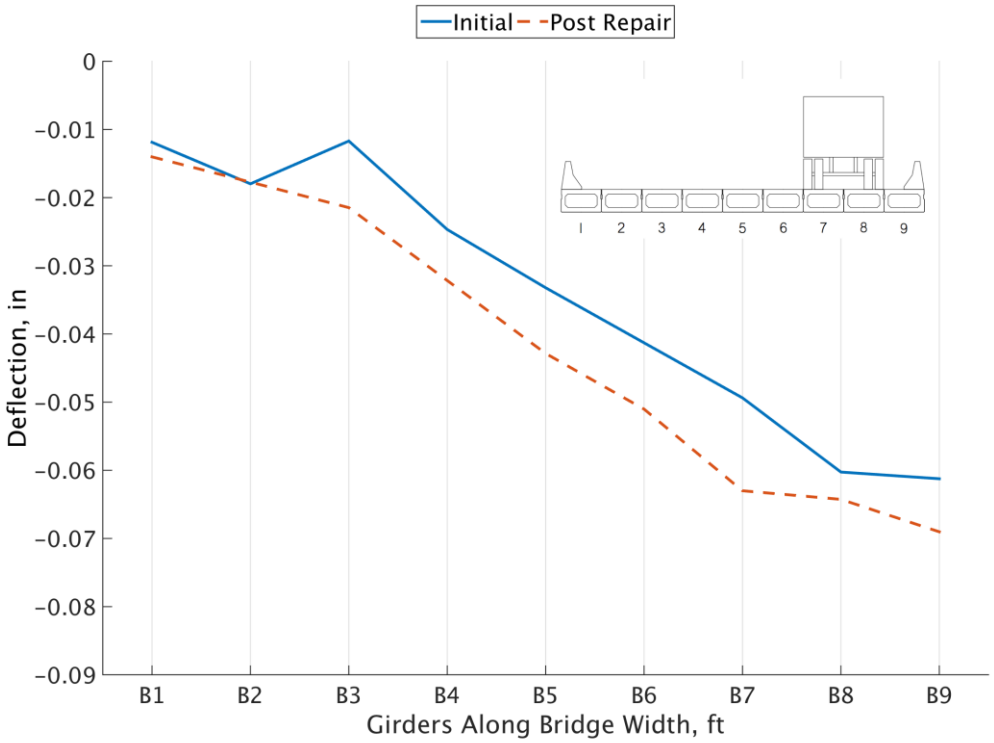

Figure 79. Load Case 4 Deflection Comparison

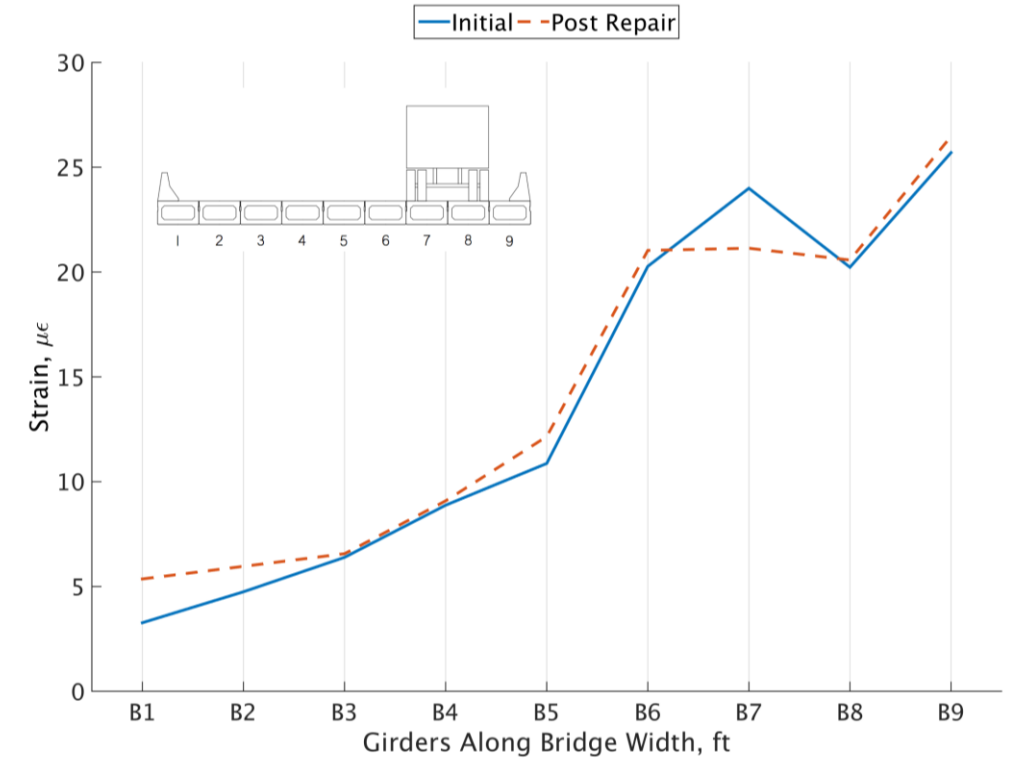

Figure 80. Load Case 4 Strain Comparison

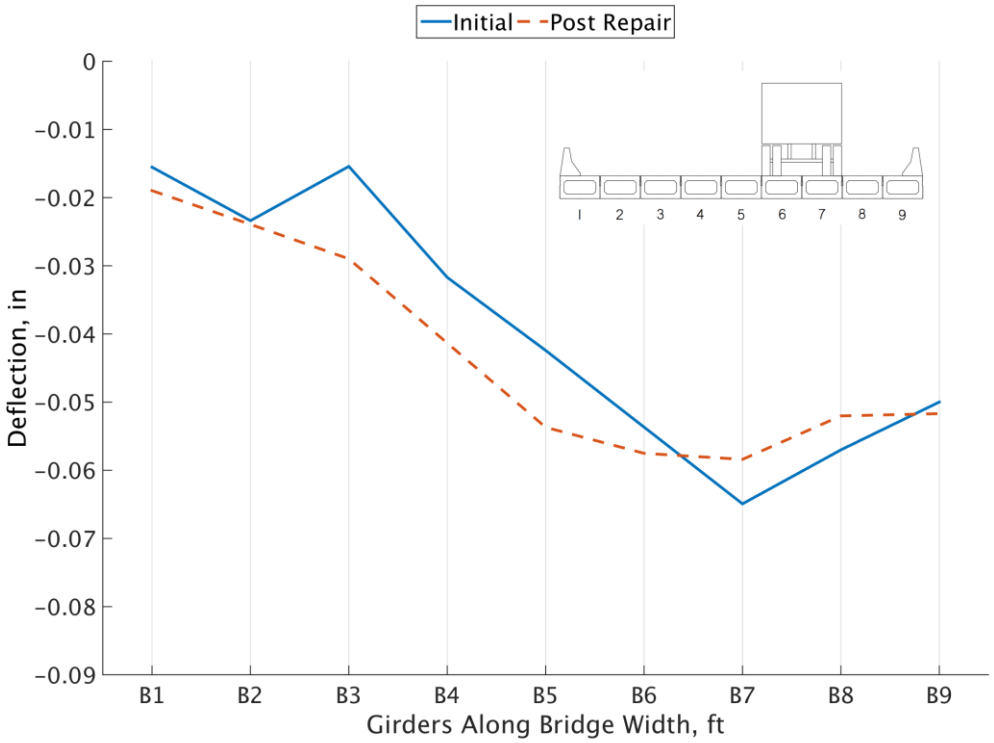

Figure 81. Load Case 5 Deflection Comparison

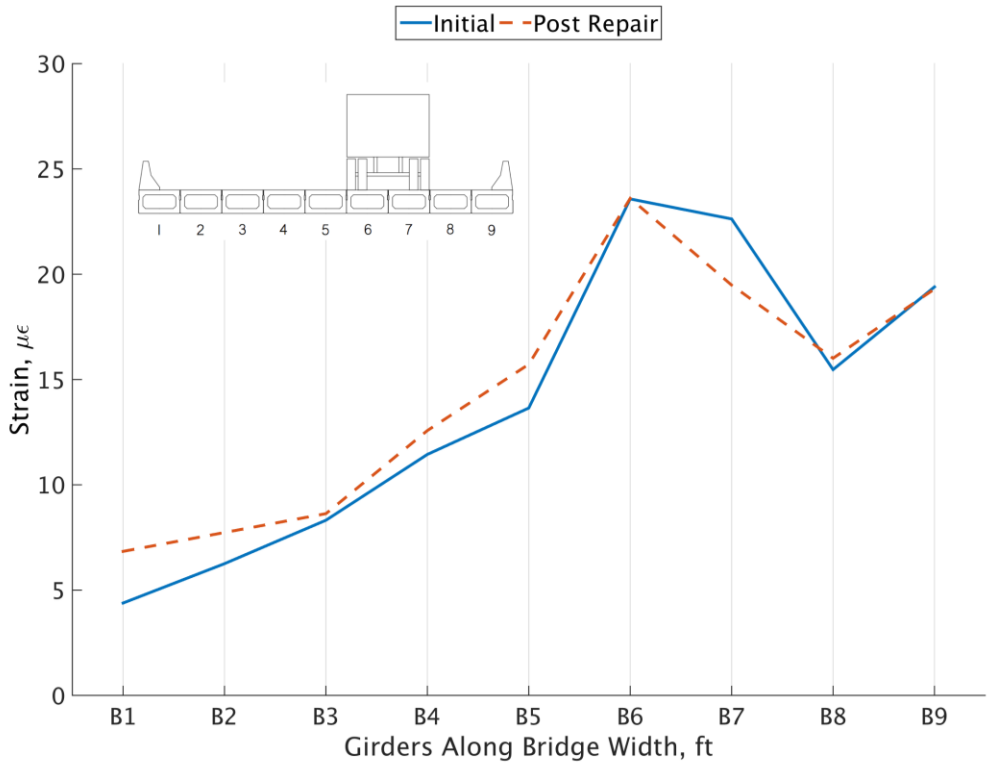

Figure 82. Load Case 5 Strain Comparison

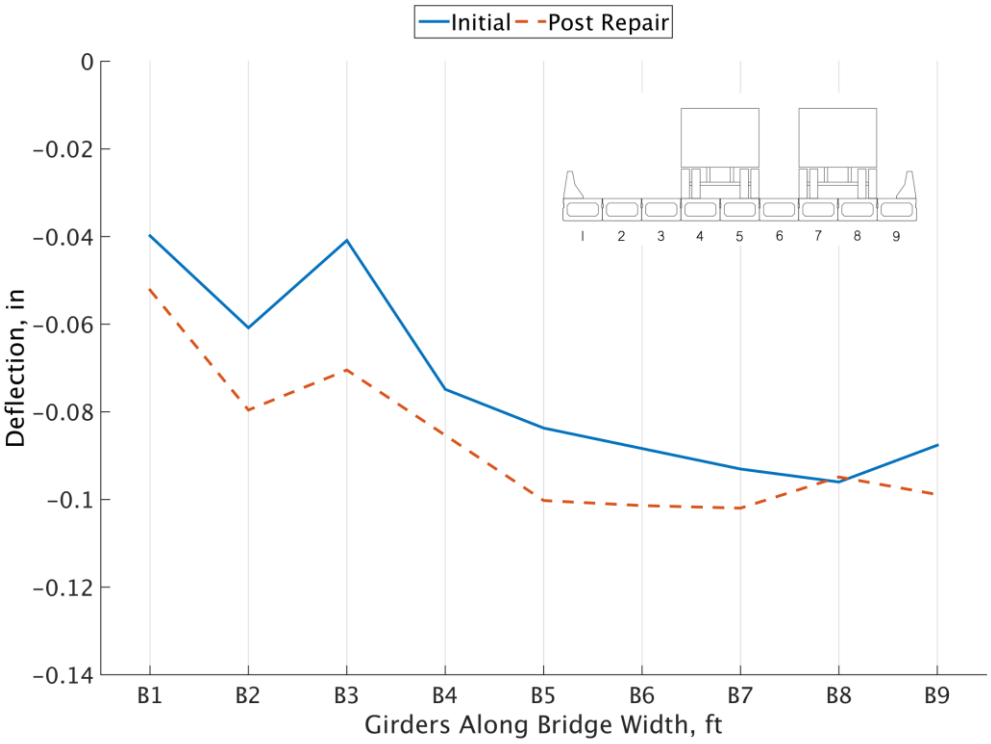

Figure 83. Load Case 6 Deflection Comparison

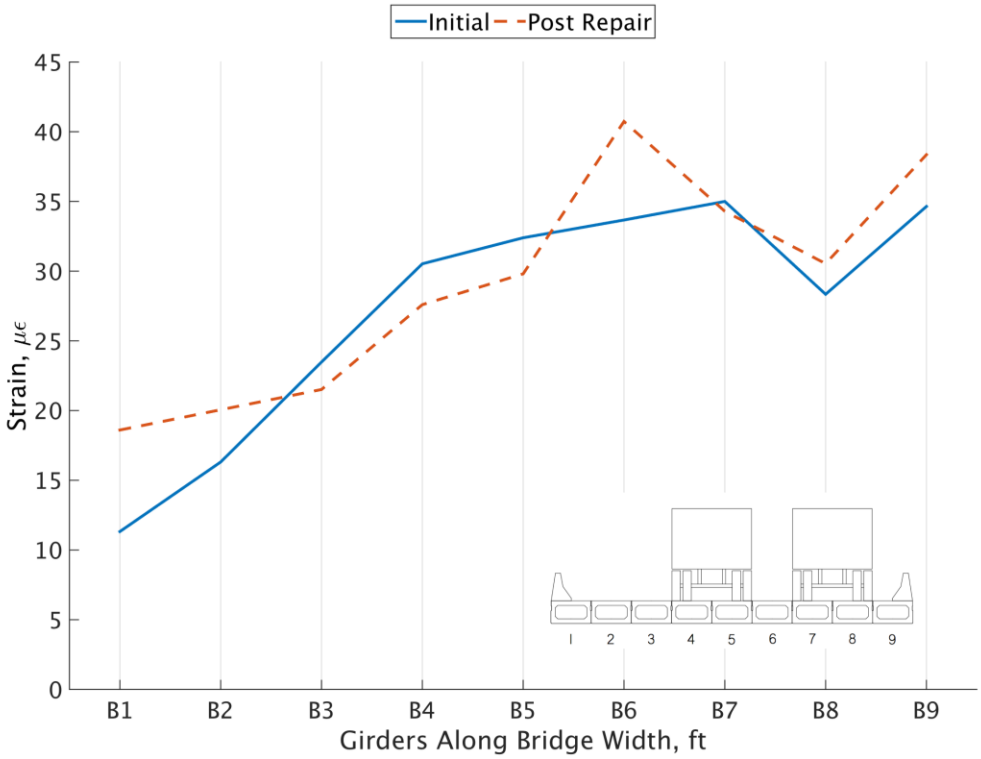

Figure 84. Load Case 6 Strain Comparison

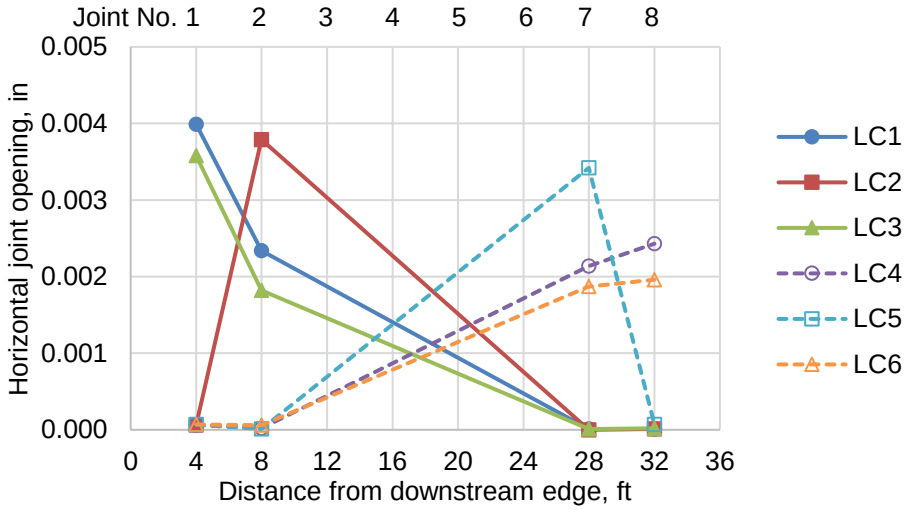

Figure 85. Relative Horizontal Displacement from Pre-Repair Test

As expected, the relative horizontal displacements for each load case generally mirrored the results of the corresponding load case with the truck on the opposite side of the bridge. In the initial test (Figure 85), the deteriorated downstream Joint 1 (between Beams 1 and 2) opened about 60% more than the upstream Joint 8 (between Beams 8 and 9), which was in relatively good condition at the time of the initial test. Post-repair, Figure 86 shows that the relative horizontal displacements at Joint 1 were smaller and similar to the relative movements in Joint 8 on the upstream side of the bridge. In both pre- and post-repair tests, Joint 2 had large horizontal displacement for LC2, in which the truck was immediately adjacent to the joint.

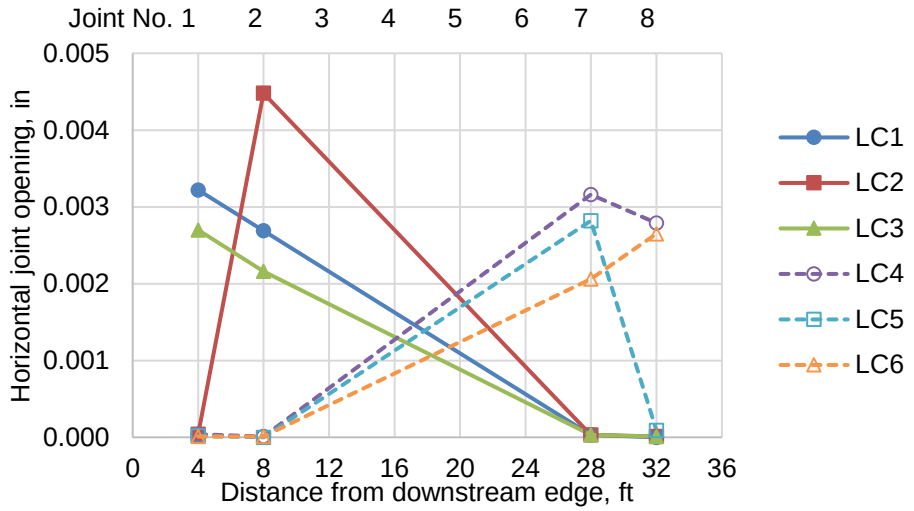

Figure 86. Relative Horizontal Displacement from Post-Repair Test

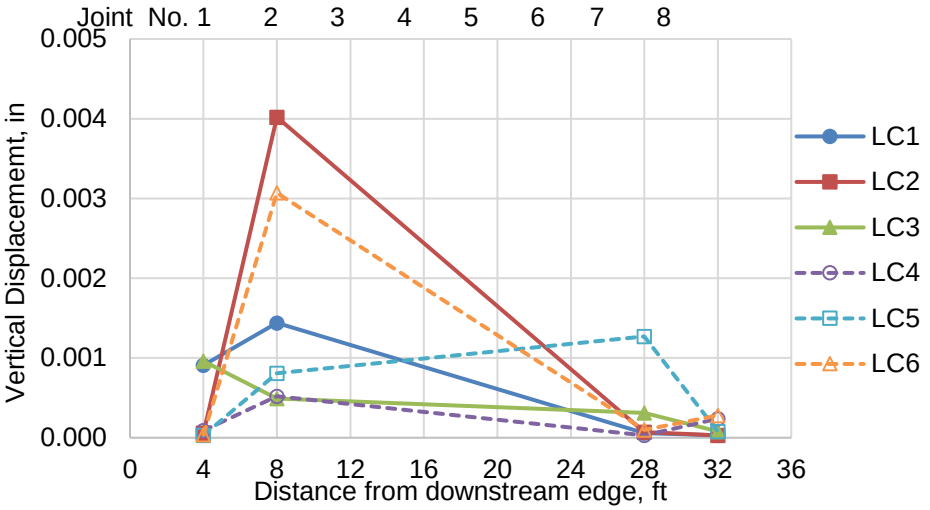

Figure 87. Relative Vertical Deflections from Pre-Repair Test

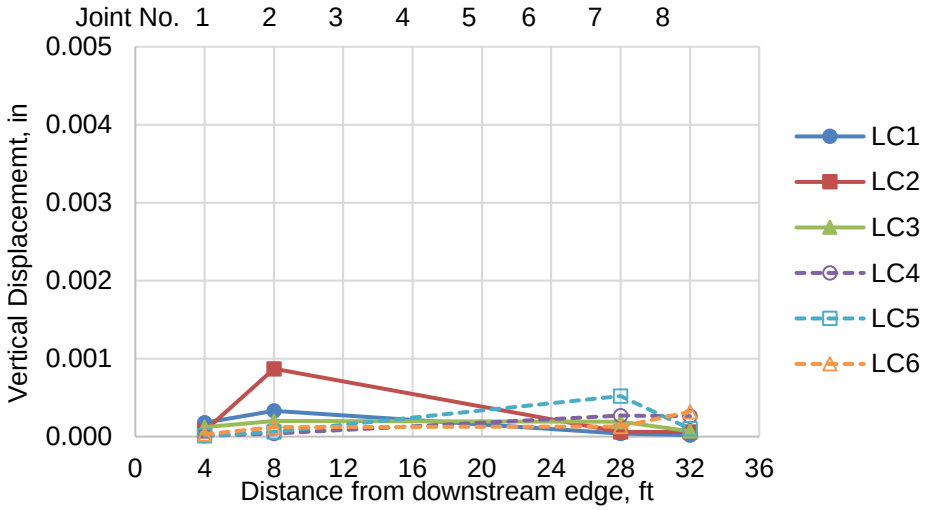

Figure 88. Relative Vertical Deflections from Post-Repair Test

There was no improvement in the horizontal joint opening after repair, indicating that the wider spacing of the dog bones may have been less effective than the smaller spacing on Joint 1.

A comparison of Figures 87 and 88 shows that the post-repair relative vertical displacements were much smaller, particularly for the joints on the downstream side of the bridge. Furthermore, the relative vertical displacements were more uniform amongst the four outermost joints. The LVDTs have a precision of 0.0001 in.

Live Load Distribution Factors

Table 17 shows the values for the Buffalo Branch Bridge used to obtain the LLDFs following the AASHTO method presented in the Methods section, and the resulting LLDFs are shown in Table 18.

Table 17. Buffalo Branch Bridge Input Values Used in AASHTO Method for Calculating Girder Distribution Factors

N_b	b, in	L, ft	I, in^4	J, in^4	d_e, ft	θ, deg
9	48	55	65941	141060	2.0	30

Table 18. LLDFs Calculated with the AASHTO Method

Load Case	Interior Girders	Exterior Girders
One Lane Loaded	0.195	0.232
Two or More Lanes Loaded	0.327	0.366

The LLDFs determined from the results of the pre-repair and post-repair live load tests are shown in Tables 19 and 20 for the case of one and two lanes loaded, respectively. To obtain these results, the LLDFs for each beam were calculated for every run of each load case. Again, outlier data from improperly functioning instrumentation was discarded, as indicated by blank cells in the table. The maximum values for each beam are presented as the LLDFs.

Table 19. LLDFs from Pre-Repair and Post-Repair Live Load Tests for One Lane Loaded

Test	Measurement	B1	B2	B3	B4	B5	B6	B7	B8	B9
Pre-Repair Test	Deflection	0.190	0.160	0.178	0.162	0.160	0.178	0.218	0.202	0.114
	Strain	0.145	0.222	0.193	0.170	0.132	0.189	0.195	0.164	0.207
Post-Repair Test	Deflection	0.192	0.194	0.165	—	0.140	0.151	0.169	0.173	0.185
	Strain	0.214	—	0.166	0.152	0.122	0.184	0.165	0.162	0.208

Table 20. LLDFs from Pre-Repair and Post-Repair Live Load Test for Two Lanes Loaded

Test	Measurement	B1	B2	B3	B4	B5	B6	B7	B8	B9
Pre-Repair Test	Deflection	0.257	0.223	0.283	0.285	0.273	0.301	0.310	0.283	0.151
	Strain	0.185	0.281	0.282	0.277	0.277	0.283	0.286	0.233	0.284
Post-Repair Test	Deflection	0.247	0.333	0.257	—	0.256	0.259	0.261	0.242	0.253
	Strain	0.266	—	0.242	0.261	0.241	0.312	0.264	0.236	0.295

Using the results from Tables 18 through 20, Figures 89 and 90 show a comparison between the AASHTO-calculated and the maximum field-assessed LLDFs for one and two or more design lanes loaded, respectively. The LLDFs obtained from all three methods were quite similar. The AASHTO method over-predicted the LLDFs, leading to a conservative design for all cases except the interior girders with one lane loaded pre-repair. The AASHTO LLDF was slightly unconservative for the interior beam when loaded with two trucks, based on the post-repair deflection data. Prior to the repair, the maximum LLDF for an interior beam determined from the load tests was 0.222 (Beam 2 in Table 19), which was 14% higher than the AASHTO calculated LLDF. Also note that the LLDF for the same case was about 12% higher when using the deflection measurements. Post-repair, those same LLDF values were 1% and 6%, respectively, *smaller* than the AASHTO result. A direct comparison of the LLDFs based on measurements and the LLDF calculated per AASHTO for the exterior beams is not entirely valid since the exterior beams were not directly loaded. However, it can be observed that all LLDFs for the exterior beams based on measurements are less than the AASHTO value. In addition, the LLDFs for the exterior beams were 1% to 3% larger post-repair compared to before the repair. Since during testing the exterior beams were never directly loaded, the increased LLDFs from measurements is an indication that the repair results in better transfer of load to the exterior beams.

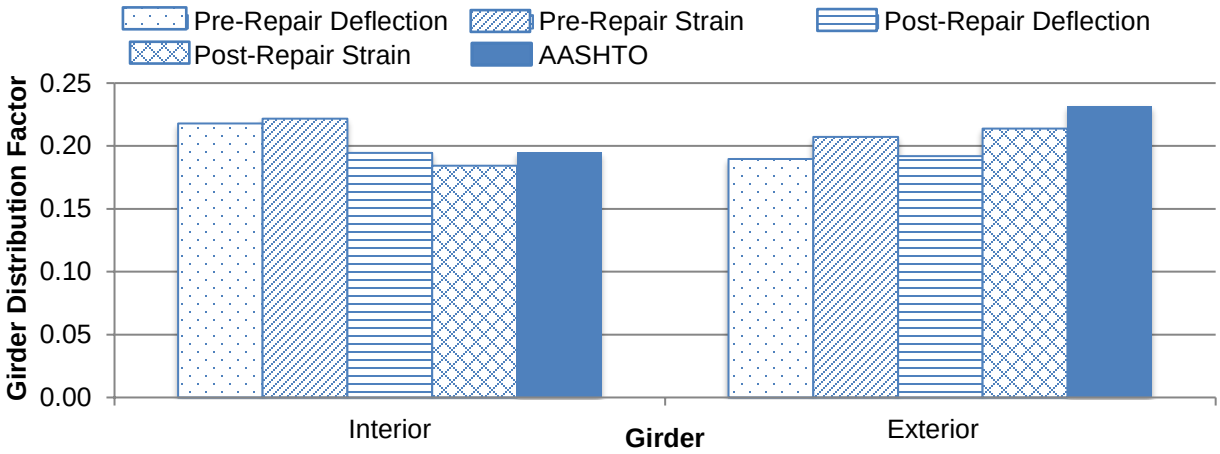

Figure 89. LLDF Comparison for One Design Lane Loaded

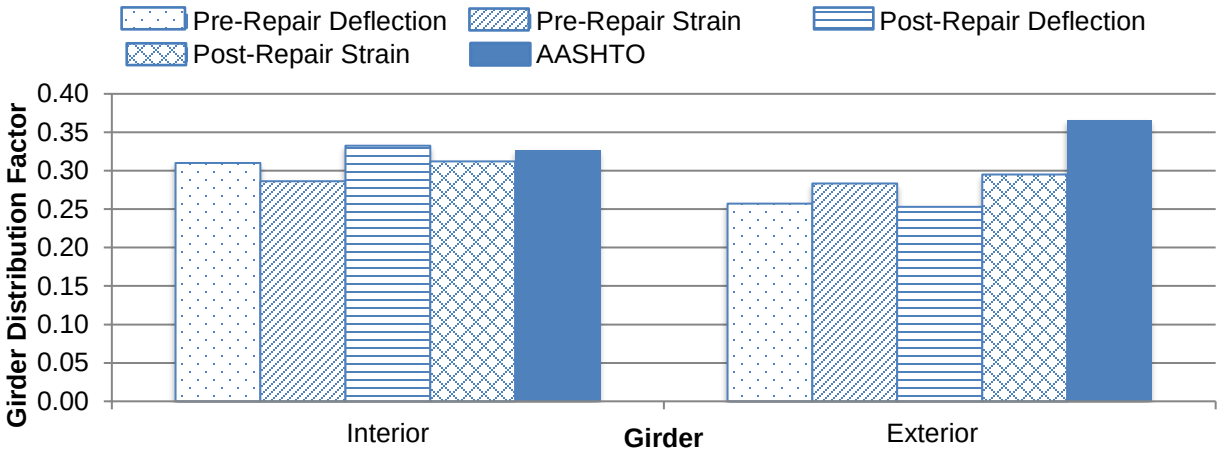

Figure 90. LLDF Comparison for Two Lanes Loaded

This section documents the rehabilitation of the Buffalo Branch Bridge, discussing variations from the original plan due to field conditions. A construction crew, consisting of two traffic flagmen, a supervisor, and six other workers performed the rehabilitation process. Several VDOT and Virginia Tech employees were also present.

Implementation of the Repair Method on Buffalo Branch Bridge

Preparing the Joints

As is common for this type of structure, every step of the rehabilitation process was completed in two stages, the downstream half followed by the upstream half, so that traffic could continue to use one lane over the bridge. The rehabilitation process began with removing the asphalt topping to expose the adjacent box beams and the joints. For the downstream half, the joints were first cleared of the existing grout and then the reinforcing steel was located, whereas for the upstream half, these two steps occurred in reverse. The grout in downstream exterior joints had severely deteriorated, closely resembling sand, and could be scooped out barehanded. However, the grout in the four interior joints was still securely bonded to the adjacent box beams and required conventional construction techniques for removal.

Although the shear keys were 12 in deep, typically only 4 in of grout was removed, as is shown in Figure 91. On the exterior joints where the grout was clearly deteriorated 4 in into the shear key, the top 4 in of the shear key was still the only grout removed because that was as deep as the jackhammer could reach into the shear key. The upstream joints were somewhat wider; therefore the jackhammer could fit up to 6 in deep.

Figure 91. Typical Depth of Cleared Joints and Removing Grout from Joints with (a) Bonded Grout and (b) Deteriorated, Sandy Grout

Locations for the cutouts were initially set at midspan and spaced from there to the end of the bridge at the planned spacings. Next, a pachometer was used to locate the reinforcing steel on both sides of each initial cutout location, as shown in Figure 92. Using the reinforcement locations, the final locations of the cutouts were marked by making short saw cuts into the adjacent box beams.

Figure 92. Locating Steel with Pachometer and Marking

Cutting the dog bones took approximately 20 minutes each, starting with coring both ends of the shape using a 3-in core drill. Next, the contractor cut the middle portion of the dog bone with a circular saw blade, chiseling out the concrete remaining in the shape. Completed dog bone cutouts are shown in Figure 93.

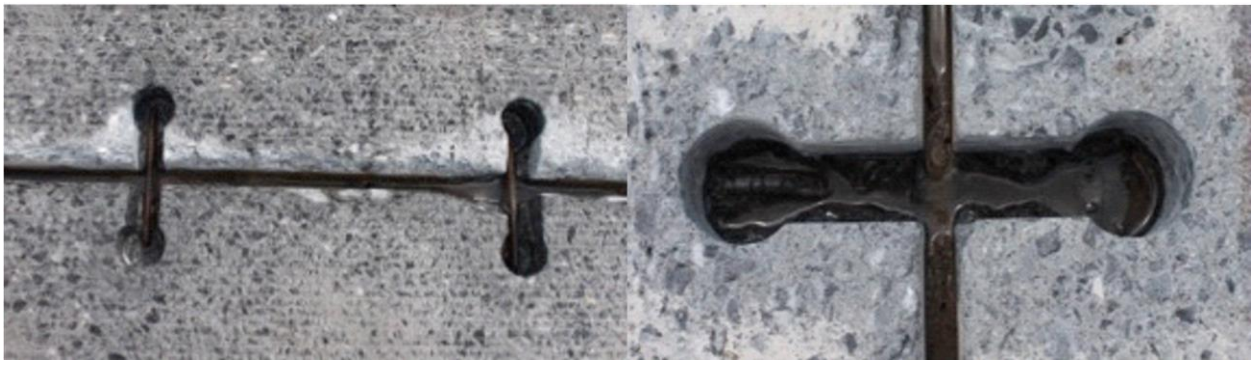

Figure 93. Dog Bones

The contractor did attempt to cut one bowtie shape at midspan of Joint 7, shown in Figure 94. Although the cutting took about the same amount of time as the dog bone, the contractor deemed that this shape was too cumbersome because the crews needed to chisel out more concrete in order to avoid cutting completely through the reinforcing steel in the precast concrete member. Thus, the rehabilitation plan was changed to using only the dog bone-shaped cutout for the non-contact splice locations. Furthermore, the plan was changed such that no additional cutouts would be made in Joint 7, and the spacing for the dog bones at Joint 8 was changed from 2 ft to 4 ft. Figure 95(a) shows Joint 1 with dog bones spaced at 2 ft and Joint 2 with dog bones spaced at 3 ft, as specified in the proposed rehabilitation plan except using dog bones instead of bowties. Figure 95(b) shows Joint 7 with only a bowtie at midspan and Joint 8 with dog bones spaced at 4 ft. Note that after cutting the pockets, the joints were sand blasted and sprayed with a hose to create a clean, SSD condition immediately before placing the VHPC.

Figure 94. Bowtie Joint

a) Joints 1 and 2 **b) Joints 7 and 8**

Figure 95. Final Configuration of Blockouts

Mixing

On the first day of placing, the contractor began mixing the first batch of VHPC at 9:30 am, with the hopes of mixing the VHPC before the ambient temperature increased to the point of affecting the working time of the VHPC. Before mixing, the contractor weighed out the required amount of each material in buckets and aligned them on a tarp with a chart outlining the materials and batch number, shown in Figure 96. Doing so allowed for the mixing process to start smoothly.

The mixing and placing procedure followed the proposed rehabilitation plan except for only using one mixer. Only one mixer was used because the joints were only cleared 4 in deep instead of 12 in, which resulted in less VHPC being needed.

After the VHPC was adequately mixed, the inverted slump test was performed to measure the spread. The original slump test from the first batch on day one of placing is shown in Figure 97(a). With a spread of 12 in, the VHPC was too stiff to place, and thus was returned to the mixer with more HRWR and some retarder added to improve the workability of the

Figure 96. Materials Pre-Weighed

(a) Day 1 First Slump **(b) Day 2 First Slump**

Figure 97. Slump Test, VHPC Too Stiff

VHPC. On the other hand, the original slump test from the first batch on day two of placing had too large a spread at 27 in. Along with the large spread, Figure 97(b) shows evidence of a mortar "halo" surrounding the VHPC. After noticing this halo effect, the materials were examined more closely. Apparently, the sand was not properly covered up overnight, when enough rain had fallen for the sand to be handled into the shape of a ball. The moisture content was determined to be 6.0%. After the amount of mix water was adjusted to compensate for this moisture, the slump tests were in line with the target spread of 18 in to 20 in, as shown in Figure 98.

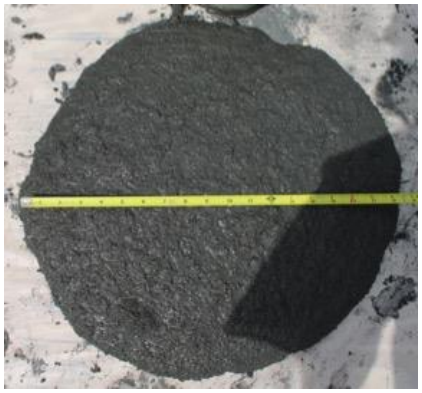

Figure 98. Slump Test, VHPC Target Spread of 18 in

The amount of HRWR and retarder that were added to each batch are presented in Table 21. The wet sand reduced the amount of HRWR and retarder that was required to achieve the target spread. The decision not to add retarder to the batches mixed on day two was also influenced by the desire to allow traffic across the rehabilitated joints in a timely manner.

Table 21. Actual HRWR and Retarder Doses

Additive	Day 1					Day 2			
	Batch 1	Batch 2	Batch 3	Batch 4	Batch 5	Batch 1	Batch 2	Batch 3	Batch 4
HRWR, oz/cwt	32	35	35	36	35	27	26	23	26
Retarder, oz/cwt	1	1	1	1	1	0	0	0	0

Placing and Curing

After the workability of the VHPC was determined to be adequate, the wheelbarrow was filled and the VHPC was dumped at the joint, shown in Figure 99.

Figure 99. Dumping VHPC from Wheelbarrow

Because the contractor did not have chairs on which to support the reinforcing steel above the existing concrete, approximately 1 in of VHPC was placed in the dog bone before the reinforcing steel was set on top of the wet concrete. The contractor then placed more VHPC up to the top of the beams, as shown in Figure 100. To prevent cold joints from forming in between batches, the construction crews rodded the VHPC where the two batches met. After placing VHPC in the entire length of the joint, the construction crew covered the joint with wet burlap for moist curing. As with conventional adjacent member bridge rehabilitation, the joints were allowed to cure overnight while the bridge was open to traffic.

On day one the downstream joints were completely placed by 12:00 pm and on day two the upstream joints were completely placed by 1:00 pm. At 5:00 pm each day, the traffic lane traveling over the newly placed joints was opened back up. Therefore, the VHPC was allowed to moist cure for five hours on day one and four hours on day two before traffic was directed back on it. Figure 101 shows the downstream joints that were placed on day one after being driven on

from 5:00 pm to the following morning. The joints did not show visual signs of damage due to exposure to traffic this soon after placing the VHPC.

Figure 100. Reinforcing Steel in Dog Bone

Figure 101. Completed Joints

Kevlar Membrane Strip and Asphalt

After curing, the contractor placed 12-inwide strips of FORTEC 5680-BD Kevlar membrane over all of the repaired joints using a two-part epoxy resin. One coat was applied to the top of the beams over the joints, and the Kevlar was pressed into the resin. Then a second coat was applied over the Kevlar. After the resin had cured, an asphalt riding surface was paved over the box beams.

Compressive and Tensile Strength of Field Cast Specimens

Figures 102 and 103 present the compressive and splitting tensile strengths of VHPC-Small used in the Buffalo Branch Bridge rehabilitation compared to the average strength of the VHPC-Small specimens cast in the laboratory. The compressive strengths were obtained by testing one cube from each batch at each age and the splitting tensile strengths were obtained by testing two of the cylinders at each age.

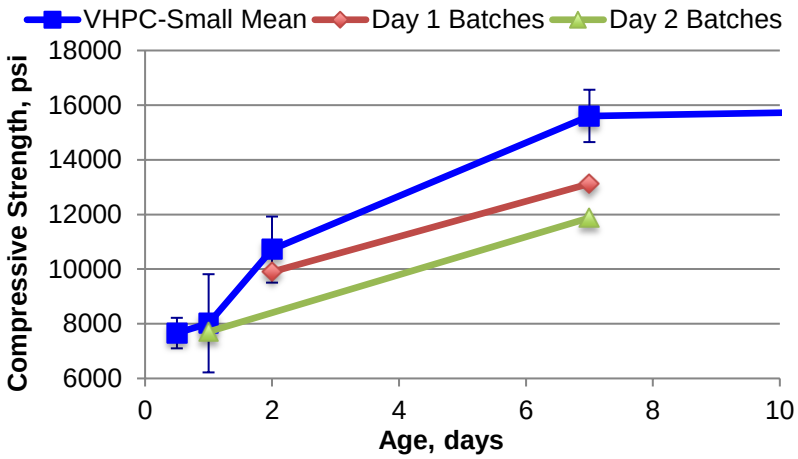

Figure 102. VHPC Compressive Strength from Bridge Rehabilitation versus Lab-mixed Samples

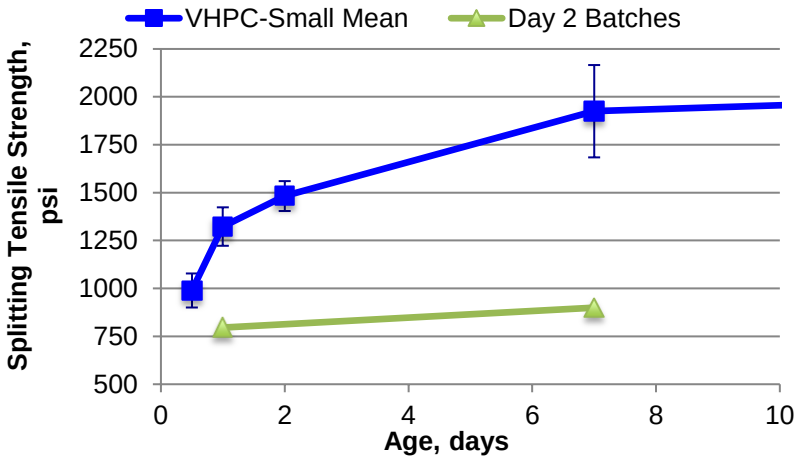

Figure 103. VHPC Splitting Tensile Strength from Bridge Rehabilitation versus Lab-Mixed Samples

CONCLUSIONS

Material Property Testing

- *UHPC and VHPC are superior to conventional grout in terms of rate of strength gain, compressive strength, splitting tensile strength, post-cracking tensile strength, lower shrinkage, and bond to the existing concrete.*

- *A workable VHPC mix can be achieved in the field.*

- *A No. 4 bar requires 5 in of embedment for VHPC that has been cured for 12 hours.*

Cyclic Tests of Non-Contact Lap Splice Connection

- *A 5-in non-contact lap splice has similar performance as a 5-in contact splice.*

Buffalo Branch Bridge Live Load Tests

- *The transfer of load to the exterior beam on the downstream side of the bridge was significantly improved after the repair, even though the rehabilitation work did not replace the existing grout from the shear key itself.*

- *Longitudinal joint repair following the proposed methods reduces the relative horizontal and vertical displacements of the adjacent members, which should result in more durable joints over time.*

- *The 2-ft center-to-center and 3-ft center-to-center cutout spacing for the exterior and first interior longitudinal joints, respectively, are adequate to improve the performance of the bridge in terms of improved load distribution and reduced relative joint displacements.*

- *The LLDFs for interior adjacent members with severely deteriorated joints, as calculated following the AASHTO design specifications, under-estimate the live loads on the adjacent members.*

- *The LLDFs for adjacent member bridges with longitudinal joints that are in good condition, as calculated following the AASHTO design specifications, are appropriately calibrated.*

Buffalo Branch Bridge Rehabilitation

- *The dog bone cutout is an achievable means of retrofitting a positive connection across the longitudinal joints in an existing adjacent member bridge.*

- *Repairing a typical bridge with the proposed retrofit joint design will take two additional days, compared with the traditional method of simply removing damaged grout from the shear key and replacing the removed material with the same type of grout.*

RECOMMENDATIONS

1. *VDOT's Structure and Bridge Division should incorporate the use of dog bone cutouts across the joints wherever practical into its guidance regarding the repair of adjacent member bridges*. Based on improved performance of the joints of the Buffalo Branch Bridge, the recommended geometry of the cutouts should be 4 in deep and should be spaced at 2 ft center-to-center for an exterior longitudinal joint and 3 ft center-to-center for interior longitudinal joints. However, absent additional research, this recommendation should be limited to bridges with skews that are 30° or less.

2. *Regarding the filler material, once a viable and dependable source for VHPC has been established, VDOT's Structure and Bridge Division should specify VHPC as the preferred material to fill the dog bone cutouts in the joints between adjacent boxes and voided slabs*.

3. *VDOT's Structure and Bridge Division should incorporate the use of a Kevlar membrane across the longitudinal joint in conjunction with the dog bone cutouts and VHPC filler material.* The Kevlar will provide additional reinforcement across the joint and additional protection from water seeping down between two adjacent members, thus further extending the service life of the structure.

4. *VDOT's Structure and Bridge Division and the Virginia Transportation Research Council (VTRC) should consider additional research to determine if the spacing in Recommendation 1 can be increased*. As previously reported, the 2-ft and 3-ft spacing for the exterior and interior joints, respectively, improved the relative displacements as well as the load transfer between adjacent members in the Buffalo Branch Bridge. Wider spacing between cutouts would be more economical, but additional research is necessary to determine if that spacing would yield acceptable performance. Among others, factors to consider should include skew, span length, and barrier conditions.

5. *VDOT's Structure and Bridge Division should consider increasing the LLDF above the AASHTO-calculated value for interior members when performing load ratings on adjacent member bridges with severely deteriorated joints*. The AASHTO LRFD Bridge Design Specifications assume interaction between adjacent members. In a deteriorated state, the degree of interaction between those members may be less than assumed. This decrease in load sharing should be accounted for when load rating such structures. "Severely deteriorated joints" are those that show signs of water leakage at the bottom of adjacent member beams along more than 50% of the length of the joint.

6. *VDOT's Structure and Bridge Division should use the AASHTO LLDF for cross-section (g) in AASHTO LRFD Bridge Design Specifications Table 4.6.2.2.1-1 when performing load ratings on adjacent member bridges with longitudinal joints that are repaired in accordance with Recommendations 1 through 3.*

IMPLEMENTATION AND BENEFITS

Implementation

The repair method presented in this report has already been successfully deployed on the Buffalo Branch Bridge. Based on the positive results of the live load testing on this structure, this method can be deployed on other structures.

However, at the time of this report, there was difficulty in obtaining the materials for the concrete mix designs similar to the VHPC prescribed in this report. VTRC has found alternative source materials. However, there are questions whether these alternatives meet the compressive, splitting tensile, and pull-out strengths of the VHPC mix design used in this study. Therefore, VTRC is currently conducting an on-going technical assistance project to answer those questions. Twelve months after a viable source for VHPC has been established, VDOT's Structure and Bridge Division will incorporate Recommendation 1 into the *Manual of the*

Structure and Bridge Division, Part 2—Design Aids and Typical Details, Chapter 32: Maintenance and Repair

Similarly, VDOT's Structure and Bridge Division will implement Recommendations 2 and 3 by revising the Special Provision for VHPC three months after a viable source for VHPC has been established.

The additional research discussed in Recommendations 4 and 5 will be considered along with other research proposals during the prioritization process established through the research advisory committees. With the advice of VDOT's Structure and Bridge Division, VTRC will evaluate the merits of sponsoring additional research after meetings of the research advisory committees and make a decision prior to the start of FY2022.

Recommendation 6 is already a part of standard practice and does not need any further implementation.

Benefits

Although somewhat more time-consuming and costly than the conventional grout repair method, the modified shear key detail using UHPC or VHPC along with reinforced dog bone cut outs should result in a much longer life span of the bridge. A longer service life will help to keep the popular and cost-effective adjacent member prestressed concrete members as a viable option in a district bridge engineer's toolbox. The savings from reduced maintenance needs for these existing structures will provide district bridge engineers more resources for other structural needs. More important, longer service intervals will decrease the frequency of road closures that temporarily restrict access to the motoring public.

ACKNOWLEDGMENTS

The authors gratefully acknowledge the guidance and assistance of Michael Brown and Bernie Kassner of VTRC and Aaron Blessing, Joshua Hall, Darrell Hayes, Rex Pearce, Marc Stecker, and Park Thompson of VDOT's Staunton District. The assistance of Ezra Bin Aref Edwin, Brett Farmer, Jimmy Grant, Kedar Halbe, Dennis Huffman, Patrick Joyce, and David Mokarem in the field and at the Murray Structural Engineering Laboratory at Virginia Tech is gratefully acknowledged.

REFERENCES

Abaqus, I. *Abaqus/Standard User's Manual.* Dassaults Systemes, Providence, RI, 2013.

Akhnoukh, A.K. *Development of High Performance Precast/Prestressed Bridge Girders.* Ph.D. Dissertation. University of Nebraska, Lincoln, NE, 2008.

American Association of State Highway and Transportation Officials. *AASHTO LRFD Bridge Design Specifications.* Sixth Edition. Washington, DC, 2012.

American Association of State Highway and Transportation Officials. *AASHTO Standard T 132-87: Tensile Strength of Hydraulic Cement Mortars.* Washington, DC, 2013.

American Institute of Steel Construction. *Manual of Steel Construction.* 14th Edition. Chicago, 2010.

ASTM International. *ASTM Standard C109/C109M: Test Method for Compressive Strength of Hydraulic Cement Mortars (Using 2-in. or [50-mm] Cube Specimens).* West Conshohocken, PA, 2013.

ASTM International. *ASTM Standard C39/C39M: Standard Test Method for Compressive Strength of Cylindrical Concrete Specimens.* West Conshohocken, PA, 2014a.

ASTM International. *ASTM Standard C469/C469M: Standard Test Method for Static Modulus of Elasticity and Poisson's Ratio of Concrete in Compression.* West Conshohocken, PA, 2014b.

ASTM International. *ASTM Standard C157/C157M: Standard Test Method for Length Change of Hardened Hydraulic-Cement Mortar and Concrete.* West Conshohocken, PA, 2014d.

ASTM International. *ASTM Standard C496/C496M: Test Method for Splitting Tensile Strength of Cylindrical Concrete Specimens.* West Conshohocken, PA, 2011.

ASTM International. *ASTM Standard C666/C666M: Standard Test Method for Resistance of Concrete to Rapid Freezing and Thawing.* West Conshohocken, PA, 2008.

ASTM International. *ASTM Standard C672/C672M-12: Standard Test Method for Scaling Resistance of Concrete Surfaces Exposed to Deicing Chemicals.* West Conshohocken, PA, 2012a.

ASTM International. *ASTM Standard D7234: Standard Test Method for Pull-Off Adhesion Strength of Coatings on Concrete Using Portable Pull-Off Adhesion Testers.* West Conshohocken, PA, 2012b.

ASTM International. *ASTM Standard C1611/C1611M: Standard Test Method for Slump Flow of Self-Consolidating Concrete.* West Conshohocken, PA, 2014c.

Collins, W.N. *Live Load Testing and Analysis of the Southbound Span of U.S. Route 15 Over Interstate-66.* M.S. Thesis. Virginia Tech, Blacksburg, 2010.

Graybeal, B. *Design and Construction of Field-Cast UHPC Connections.* FHWA-HRT-14-084. Federal Highway Administration, McLean, VA, 2014.

Halbe, K.R. *New Approach to Connection Details Between Adjacent Box Beam Bridges.* Ph.D. Dissertation. Virginia Tech, Blacksburg, 2014.

Halbe, K.R., Field, C.S., Cousins, T.E., and Roberts-Wollmann, C.L. *Improved Connection Details for Adjacent Prestressed Bridge Beams,* CAIT-UTC-001, Center for Advanced Infrastructure and Transportation, Rutgers, Piscataway, NJ, 2015.

Home Depot. Cement and Concrete Aggregates. https://www.homedepot.com/p/Quikrete-50-lb-Non-Shrink-Precision-Grout-158500/100318529. Accessed December 27, 2017.

Johnson, J.B. *Bond Strength of Corrosion Resistant Steel Reinforcement in Concrete.* M.S. Thesis. Virginia Tech, Blacksburg, 2010.

Joyce, P.C. *Development of Improved Connection Details for Voided Slab Bridges.* M.S. Thesis. Virginia Tech, Blacksburg, 2014.

Lane, D.S., and Ozyildirim, C. *Combinations of Pozzolans and Ground, Granulated, Blast-Furnace Slag for Durable Hydraulic Cement Concrete.* VTRC 00-R1. Virginia Transportation Research Council, Charlottesville, 1999.

Scholz, D.P., Wallenfelsz, J.A., Lijeron, C., and Roberts-Wollmann, C.L. *Recommendations for the Connection Between Full-Depth Precast Bridge Deck Panel Systems and Precast I-Beams.* VTRC 07-CR17. Virginia Transportation Research Council, Charlottesville, 2007.

Virginia Department of Transportation. *Road and Bridge Specifications.* Richmond, 2007.

Virginia Department of Transportation. *Manual of Structure and Bridge Division,* Volume V. Richmond, 2015.